





Criminal Behavior in Frontotemporal Dementia: A Multimodal MRI Study

Karsten Mueller¹ | Nico Scherf¹ | Timo Grimmer² | Janine Diehl-Schmid² | Adrian Danek³ | Johannes Levin³ | Jens Wiltfang⁴ | Sarah Anderl-Straub⁵ | Markus Otto⁶ | Matthias L. Schroeter^{1,7} | FTLD Consortium Germany

¹Max Planck Institute for Human Cognitive and Brain Sciences, Leipzig, Germany | ²Department of Psychiatry and Psychotherapy, Technical University Munich, München, Germany | ³Department of Neurology, LMU University Hospital, LMU Munich, München, Germany | ⁴Department of Psychiatry and Psychotherapy, Medical University Göttingen, Göttingen, Germany | ⁵Department of Neurology, University of Ulm, Ulm, Germany | ⁶Department of Neurology, University Hospital Halle (Saale), Halle (Saale), Germany | ⁷Clinic of Cognitive Neurology, University Hospital Leipzig, Leipzig, Germany

Correspondence: Karsten Mueller (karstenm@cbs.mpg.de)

Received: 16 December 2024 | Revised: 17 April 2025 | Accepted: 25 July 2025

Funding: The authors received no specific funding for this work.

Keywords: behavioral variant frontotemporal dementia | brain imaging | criminal behavior | disinhibition | frontotemporal lobar degeneration | magnetic resonance imaging | temporal lobe

ABSTRACT

The behavioral variant of frontotemporal dementia (bvFTD) is related to a variety of social misbehaviors, including criminal behavior (CB) due to deep changes in cognition, behavior, and personality. Recent work suggests that impairment in emotional processing, along with disinhibition, constitutes the necessary elements for CB in bvFTD. However, the underlying neurobiological mechanisms are still unclear. Therefore, we aim at investigating structural and functional brain changes related to CB in bvFTD using magnetic resonance imaging (MRI) with the German Consortium for Frontotemporal Lobar Degeneration (FTLD). Our study comprised 87 patients with bvFTD and 26 healthy controls recruited within different locations of the FTLD Consortium. A subset of 21 patients with bvFTD showed CB, including theft, physical violence, sexual assault, drug abuse, and violations against traffic law. Voxel-based morphometry was performed, generating gray matter density (GMD) images obtained from high-resolution T1-weighted MR images. In addition, surface-based morphometry was performed by reconstruction of cortical thickness using a projection-based thickness approach. Both GMD and cortical thickness were further analyzed in order to detect group differences between bvFTD with and without CB. Resting-state functional MRI was available for a subgroup of 56 patients with bvFTD, including 16 patients showing CB. On a behavioral level, CB in bvFTD was associated with a higher frequency of disinhibition, lower frequency of apathy, and better performance in verbal fluency. Comparing bvFTD with and without CB, we obtained reduced GMD and reduced cortical thickness in the temporal lobe, predominantly in the left hemisphere. Impairment in brain structure was correlated with the Frontal Systems Behavior Scale, particularly with disinhibition, in the left superior temporal gyrus in interaction with CB in bvFTD. Investigating functional MRI data, CB was associated with significant functional brain dysconnectivity, particularly between the left anterior superior temporal gyrus and widely distributed cortical regions, including areas in the vicinity of the precentral sulcus and the inferior frontal junction, related to executive functions. Our study revealed structural and functional brain differences between bvFTD with and without CB, showing CB-related reduced GMD and cortical thickness in the left temporal lobe, indicating disinhibition as the main driver for CB. Interestingly, brain degeneration in the temporal lobe is discussed with CB in bvFTD in the current literature, dominantly affecting the right hemisphere. Our study investigates specifically the neural correlates of CB in bvFTD with MRI, modifying this view. Further work is necessary to shed more light on the role of the temporal lobe in bvFTD with CB.

This is an open access article under the terms of the Creative Commons Attribution-NonCommercial-NoDerivs License, which permits use and distribution in any medium, provided the original work is properly cited, the use is non-commercial and no modifications or adaptations are made.

© 2025 The Author(s). Human Brain Mapping published by Wiley Periodicals LLC.

Summary

- Criminal behavior in frontotemporal dementia is related to brain structure alterations in the left and right temporal lobes.
- Disinhibition is correlated with reduced gray matter density and cortical thickness in the temporal lobe, specifically in patients showing criminal behavior.
- Comparing patients with and without criminal behavior, functional brain connectivity decrease was obtained between regions of the temporal and frontal lobes.

1 | Introduction

Frontotemporal dementia (FTD) or frontotemporal lobar degeneration (FTLD) is a complex neurological disease that affects the frontal and temporal lobes of the brain, regions crucial for controlling behavior, emotion, and language (Rascovsky et al. 2011). Unlike other forms of dementia, which typically affect memory first, the behavioral variant of FTD (bvFTD) manifests in changes in personality, behavior, executive, and socioemotional cognitive functions, combined with social and criminal transgressions (Mendez 2022; Mendez, Anderson, and Shapira 2005; Schroeter et al. 2014). Among the behavioral changes, criminal behavior (CB) in individuals with bvFTD has emerged as a particularly challenging aspect for persons affected, families, and healthcare providers. CB may include shoplifting, physical aggression, sexual misconduct, or other actions that are out of character for the individual and can lead to legal issues (Mendez 2022). The loss of social norms and impulse control, common in bvFTD, contributes to these behaviors. Caregivers often find themselves in difficult positions, needing to navigate the legal system while advocating for their loved ones who do not fully comprehend the consequences of their actions due to frequent anosognosia. This situation underscores the importance of early diagnosis, tailored interventions, and support systems for both patients and their families to manage these complex challenges effectively (Caceres et al. 2016). While not all individuals with bvFTD engage in CB, there is a notable prevalence of such actions compared to other forms of dementia (Diehl-Schmid et al. 2013; Liljegren et al. 2019; Shinagawa et al. 2017). Brain imaging techniques play a crucial role in diagnosing FTD by providing detailed images of the brain's structure, allowing for the observation of atrophy and/ or hypoperfusion/hypometabolism in the frontal and temporal lobes (Rosen, Gorno-Tempini, et al. 2002; Whitwell 2019). In particular, Magnetic Resonance Imaging (MRI) helps differentiate bvFTD from other types of FTD and other forms of neurodegenerative disease through its non-invasive, high-resolution imaging capabilities, enabling early diagnosis and the possibility of managing symptoms more effectively and as early as possible (Meyer et al. 2017). However, there is no imaging study so far differentiating bvFTD with and without CB.

Interestingly, the temporal lobe shows a relevant involvement with CB, which was found particularly with murderers (Gatzke-Kopp et al. 2001) and criminal psychopaths (Kiehl et al. 2004).

Using voxel-based morphometry (VBM), antisocial behavior was associated with a decrease of gray matter volume of the temporal lobe, showing a link between gray matter decrease and the level of reactive aggression (Hofhansel et al. 2020). A lesion-based association study also demonstrated a significant impairment of regions within the temporal lobe in CB (Darby et al. 2018). Thus, the temporal lobe's involvement seems to be relevant when considering CB. The temporal lobe is involved in various functions critical to human behavior and interaction. The hippocampus is essential for memory formation, whereas the amygdala plays a key role in emotion processing. The temporal lobe also contributes to language comprehension, facial recognition, and sensory processing. These functions collectively enable individuals to navigate social environments, make decisions based on past experiences, and regulate emotional responses. The emergence of CB in individuals with bvFTD can be partly attributed to temporal lobe dysfunction (Mendez 2022). The impaired emotional processing and reduced empathy resulting from temporal lobe damage can lead to a lack of understanding of social norms and the consequences of one's actions (Rosen et al. 2005; Seeley 2008). Additionally, the loss of impulse control, a symptom associated with both frontal and temporal lobe damage, may result in aggressive or inappropriate behavior (Mendez 2022). Moreover, disinhibition—a frequent behavioral symptom in bvFTD—has specifically been related to (mainly left) temporopolar hypometabolism, beside the amygdala, insula, and orbitofrontal areas (Schroeter et al. 2011). Notably, recent studies showed socially undesirable behavior as an initial symptom (including CB) (Mychack et al. 2001) and sociopathic acts (Mendez, Chen, et al. 2005) mainly in right-lateralized bvFTD, and bilateral frontomedian atrophy being associated with antisocial behavior in a diverse dementia cohort including bvFTD (Phan et al. 2023). Thus, an impairment of the temporal and frontal lobe is a major hallmark of assessing CB in bvFTD; however, there is no study consistently comparing bvFTD with and without CB using structural and functional MRI.

The major aim of our study is to further investigate neural correlates of CB in bvFTD. We will particularly analyze structural gray matter density and cortical thickness changes associated with CB across the whole brain. In a second step, we will investigate brain connectivity alterations from atrophic areas. Analyses are based on the large cohort of the German FTLD Consortium. We expect gray matter density decline, reduction of cortical thickness, and connectivity changes with CB particularly in the (pre)frontotemporal lobes. In addition, findings of the structural MRI analysis will be related to behavioral dysfunction applying the Frontal Systems Behavior Scale (FrSBe) (Grace and Malloy 2020; Stout et al. 2003) using all subscales encoding executive dysfunction, disinhibition, and apathy, which represent central and characteristic alterations in bvFTD (Schroeter et al. 2012, 2011; Weise et al. 2024). Note that all structural assessments will be performed on the voxel- and vertex-level but also using region-based analysis with the LONI Probabilistic Brain (Shattuck et al. 2008) and the Desikan-Killiany (Desikan et al. 2006) atlas. As both approaches are eventually dealing with the same data just averaging voxels within regions with the atlas-based method, we expect a high degree of concordance between the voxel-/ vertex-wise and region-based analyses.

2 | Materials and Methods

2.1 | Patient Cohort

The study aimed at investigating patients showing CB in bvFTD using data from the multi-centric German FTLD consortium conducted in Germany since 2011 (*N*=1711; Date: October 8, 2024; http://www.ftld.de). For detailed information regarding the study's protocol, please refer to (Otto et al. 2011). Clinical evaluation, neuropsychological assessments, and MRI have been performed within centers of the FTLD Consortium according to strict standard operating procedures (SOPs). Among several parameters obtained, clinicians—that is experienced psychiatrists and/or neurologists—had to state whether CB was present. Information was based on careful clinical and neuropsychological examination, case history including reports by relevant others, that is, caregivers, relatives, spouses, and thorough characterization with questionnaires on behavior, cognitive function, and everyday live activities.

Among all patients of the multi-centric German FTLD consortium, a subset of 475 patients was diagnosed with bvFTD. High-resolution structural MRI data were available for 87 patients with bvFTD, including 21 patients showing CB (further denoted as "CB-bvFTD") and 66 patients showing no signs of CB (further denoted as "NoCB-bvFTD") based on the aforementioned criteria. A patient selection scheme is shown in Figure 1.

Patients were included at the centers of the FTLD Consortium Göttingen, Leipzig, Ulm, and Munich. For patients showing bvFTD, further information was obtained for the type of CB from clinicians/M.D.s, who screened medical records. The most frequent type of CB was theft (17/21) but it also included CB related to physical violence (4/21) and sexual assault (4/21). In addition to these violations, patients also showed alcohol and drug abuse (4/21) and violations against traffic law (8/21). Although the type of CB was known for each patient, a CB severity score was not available. Functional MRI data were obtained for a subgroup of 56 patients with bvFTD, including 16 patients with CB. In addition to patients with bvFTD, 26 healthy controls (HC) were obtained from the German FTLD consortium to match the 21 patients with bvFTD showing CB. Healthy controls were collected by scanning healthy family members (non-consanguine) or other healthy participants within the same age group.

For all participants, demographic and clinical details are listed in Table 1. Cognitive assessment was performed according to the neuropsychological test battery of the Consortium to Establish a Registry for Alzheimer's Disease (CERAD) (Morris et al. 1989). For all patients with bvFTD, Table 2 lists clinical behavioral alterations incorporated into the diagnostic criteria according to the international consensus criteria for bvFTD (Rascovsky et al. 2011). In addition, behavioral impairment was assessed—embedded into the general battery of the FTLD consortium—with the Frontal Systems Behavior Scale (FrSBe)

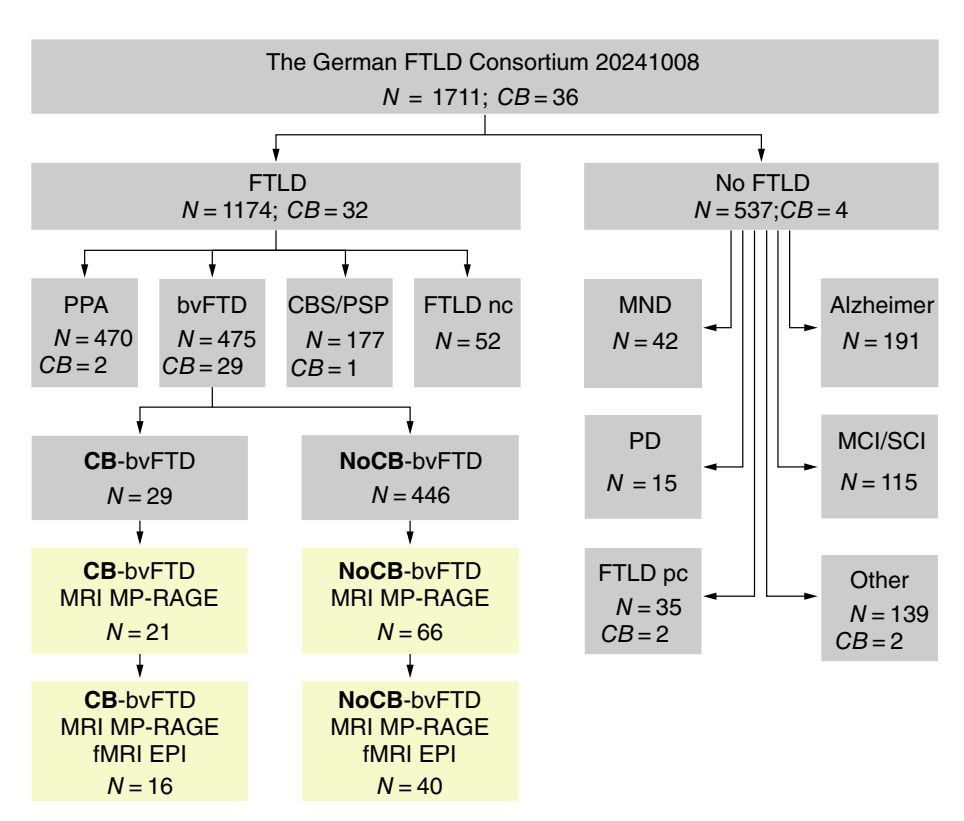


FIGURE 1 | Patient selection scheme using all data of the German Consortium for Frontotemporal Lobar Degeneration (FTLD) obtaining patients with and without criminal behavior (CB) in the behavioral variant of frontotemporal dementia (bvFTD). Finally, high-resolution structural MRI data were available for 87 patients with bvFTD including 21 patients showing CB (CB-bvFTD) and 66 patients showing no signs of CB (NoCB-bvFTD). CBS—corticobasal syndrome, MCI—mild cognitive impairment, MND—motor neuron disease, NC—not classified, PC—phenocopy, PD—Parkinson's disease, PPA—primary progressive aphasia, PSP—progressive supranuclear palsy, SCI—subjective cognitive impairment.

TABLE 1 | Demographic and clinical characteristics of patients with bvFTD and healthy controls.

	CB-bvFTD	NoCB-bvFTD	HC	P (CB, NoCB)	р
N	21	66	26		
Gender (f/m)	7/14	32/34	13/13		
Age (years)	64.2 ± 11.2	62.5 ± 9.4	63.6 ± 11.5	0.530	0.756
Education (years)	14.6 ± 3.3	13.1 ± 2.8	14.4 ± 2.8	0.068	0.056
B-ADL	5.5 ± 2.4	5.8 ± 2.3		0.606	
Disease duration	3.8 ± 4.3	4.0 ± 4.5		0.919	
MMSE	24.7 ± 5.1	23.9 ± 5.0	29.0 ± 1.0	0.531	< 0.001
CDR	5.8 ± 3.8	5.7 ± 3.2	0.1 ± 0.3	0.854	< 0.001
FTLD-CDR	8.1 ± 4.7	7.8 ± 4.0	0.1 ± 0.3	0.796	< 0.001
CERAD: verbal fluency	16.3 ± 8.0	10.6 ± 5.9	23.7 ± 4.8	0.010	< 0.001
CERAD: Boston naming	12.0 ± 3.1	12.4 ± 2.9	14.7 ± 0.5	0.658	0.001
CERAD: word list recall	4.5 ± 3.0	4.4 ± 2.5	8.4 ± 2.0	0.865	< 0.001
CERAD: figure recall	5.5 ± 3.8	5.4 ± 3.5	9.6 ± 2.1	0.926	< 0.001
CERAD: trail making test A	69.5 ± 47.1	77.3 ± 39.5	38.3 ± 15.5	0.540	< 0.001
CERAD: phonemic fluency	9.3 ± 6.2	6.6 ± 4.8	17.2 ± 4.6	0.112	< 0.001

Note: p-values within the last column were obtained using a single-factor ANOVA including an alpha level of 0.05. Although a significant increase of verbal fluency was obtained in CB-bvFTD, compared with NoCB-bvFTD, there is still a significant distance of verbal fluency between CB-bvFTD and HC (p=0.002). Abbreviations: B-ADL-Bayer activities of daily living scale; bvFTD-behavioral variant of frontotemporal dementia; CB-bvFTD and NoCB-bvFTD-group of bvFTD with and without CB; CB-criminal behavior; CDR-clinical dementia rating scale; CERAD-Test battery of the Consortium to Establish a Registry for Alzheimer's Disease; f-females; FTLD-frontotemporal lobar degeneration; HC-healthy controls; m-males; MMSE-mini mental state examination; p (CB, NoCB)-values were obtained using a two-samples t-test with unequal variances comparing groups of bvFTD with and without CB (two-tailed).

(Grace and Malloy 2020; Stout et al. 2003) for a subset of 66 patients with bvFTD including 13 patients showing CB (Table 3). This behavioral scale provides a brief, reliable, and valid measure of three frontal systems behavioral syndromes: apathy, disinhibition, and executive dysfunction. It includes a total score and subscales related to the three frontal syndromes. We used a modified FrSBe (Grace and Malloy 2020) version that quantifies frequency and distress of all three behavioral categories obtained by the statements of the patient's companion. The study was conducted following the Declaration of Helsinki and approved by the local ethics committees (Ethics Committee University Leipzig ID 137-11-18042011, University of Ulm ID #39/11). Participants provided written informed consent.

2.2 | Other Patient Cohorts

Among all patients of the FTLD consortium, a subgroup of patients was detected showing right anterior temporal lobe (RATL) predominance (Ulugut et al. 2024). Assessment for a potential RATL predominance was performed using a visual rating scale in order to evaluate brain degeneration in the left and right frontal and temporal lobes (Kipps et al. 2007). Patients showing RATL prominence were detected according to the guidelines of the international right temporal variant FTD working group: "The most important issue is that the frontal or the left temporal atrophy scores must be lower (at least 1 grade) than the RATL atrophy score." According to these criteria, only 24 patients were found within the whole FTLD data base showing an RATL dominance. Among these 24 patients, only a single patient showed

CB. High-resolution structural MRI data were available for 22 patients, resulting in a final group of 21 patients showing RATL predominance excluding the patient showing CB.

A further subgroup from all FTLD patients was obtained by selecting all patients showing primary progressive aphasia (PPA, N=470) (Gorno-Tempini et al. 2011). Within this group, patients were selected showing the semantic variant of PPA (svPPA, N=119). Among these 119 patients with svPPA, two patients showed CB. High-resolution structural MRI data were available for 60 patients, resulting in a final group of 58 patients showing svPPA, excluding two patients showing CB.

2.3 | Structural MRI Data Pre-Processing

High-resolution structural T1-weighted images were obtained using the magnetization prepared rapid gradient-echo (MP-RAGE) (Mugler 3rd and Brookeman 1991) sequence. All structural images were processed using VBM (Ashburner and Friston 2000, 2001) with the Computational Anatomy Toolbox (CAT) (Gaser et al. 2023) rev. 12.8.2 (Structural Brain Mapping Group, Department of Neurology, Jena University Hospital, Germany) and Statistical Parametric Mapping (SPM) (Friston et al. 2007) 12 rev. 7771 (Functional Imaging Laboratory, UCL Queen Square Institute of Neurology, London, UK) with Matlab 9.13 rev. 2022b (The MathWorks Inc.). All structural images were processed within the CAT toolbox (Gaser et al. 2023) using an initial denoising with a spatial adaptive non-local means (SANLM) denoising filter (Manjon et al. 2010). Thereafter,

TABLE 2 | Diagnostic criteria for the behavioral variant of frontotemporal dementia (ves/no).

TABLE 3 | Demographic and clinical characteristics of patients with byFTD including FrSBe values.

trontotemporal dementia (yes/no).				byFTD including FrSBe values.					
	CB- bvFTD	NoCB- bvFTD	p		CB-bvFTD	NoCB- bvFTD	p		
N	21	66		N	13	53			
A.1. Disinhibition: Socially inappropriate behavior	18/3	34/32	0.005	Gender (f/m)	5/8	27/26			
				Age (years)	67.7 ± 8.8	62.9 ± 9.3	0.098		
A.2. Disinhibition: Loss of manners or decorum	15/6	31/35	0.078	Education (years)	13.8 ± 2.6	12.9 ± 2.9	0.277		
A.3. Disinhibition: Impulsive, rash or careless actions	18/3	40/26	0.037	MMSE	23.3 ± 5.6	23.5 ± 5.3	0.891		
				Disease duration	4.9 ± 5.1	3.8 ± 3.8	0.469		
				CDR	6.8 ± 4.4	5.6 ± 3.3	0.398		
B.1. Apathy	11/10	52/14	0.026	FTLD-CDR	9.3 ± 5.5	7.8 ± 4.1	0.388		
B.2. Inertia	10/11	40/26	0.321	FrSBe: Total (f)	77.6 ± 14.2	73.1 ± 15.2	0.325		
C.1. Diminished response to people's needs and feelings	16/5	45/21	0.590	FrSBe: Total (d)	66.6 ± 16.0	60.6 ± 17.6	0.274		
C.2. Diminished social interest or personal warmth	15/6	43/23	0.791	FrSBe: Executive (f)	27.8 ± 6.1	27.1 ± 6.1	0.691		
				FrSBe: Executive (d)	22.1 ± 6.7	21.6 ± 6.6	0.829		
D.1. Simple repetitive movements	5/16	8/58	0.289	FrSBe: Disinhibition (f)	19.9 ± 6.3	16.8 ± 6.5	0.133		
D.2. Complex, compulsive or ritualistic behaviors	5/16	17/49	1.000	FrSBe: Disinhibition (d)	18.1 ± 5.2	15.2 ± 6.5	0.111		
D.3. Stereotypy of speech	6/15	9/57	0.181	FrSBe: Apathy (f)	29.8 ± 4.6	28.6 ± 7.6	0.452		
E.1. Altered food	12/9	29/37	0.325	FrSBe: Apathy (d)	25.8 ± 7.0	22.9 ± 8.1	0.226		
preferences				Note: p-values were obtained u	sing a two-samples t	test with unequa	l variances		
E.2. Binge eating, increased consumption of alcohol	8/13	17/49	0.283	(two-tailed). Abbreviations: (d)—distress; (f)—frequency; bvFTD—behavioral variant of frontotemporal dementia; CB-bvFTD and NoCB-bvFTD—group of bvFTD with and without CB; CB—criminal behavior; CDR—clinical dementia rating scale;					
E.3. Oral exploration or consumption of inedible objects	2/19	3/63	0.590	f—females; FrSBe—Frontal Systems Behavior Scale; FTLD—frontotemporal lobar degeneration; m—males; MMSE—mini mental state examination.					

using a spatial Gaussian filter with 8 mm full-width at half maximum (FWHM) and fed into subsequent voxel-wise statistical analysis (Ashburner and Friston 2000).

In addition to voxel-based processing, surface-based analysis was performed with the CAT toolbox estimating cortical thickness using a projection-based thickness (PBT) approach (Dahnke et al. 2013). This PBT approach handles partial volume effects, sulcal blurring, and sulcal asymmetries without explicit sulcus reconstruction (Dahnke et al. 2013). Surface reconstruction was refined, correcting for topological inconsistencies using spherical harmonics (Yotter, Dahnke, et al. 2011). Individual surface reconstructions were subsequently spatially normalized using FreeSurfer's FsAverage template (Fischl et al. 1999) using a spherical mapping with minimal distortions (Yotter, Nenadic, et al. 2011), and cortical thickness values were mapped onto the FsAverage template. Prior to vertex-wise statistical analysis, spatial smoothing was applied using a Gaussian filter with a suggested kernel size of 15 mm FWHM.

Voxel- and surface-based analysis was also accompanied by region-based analysis, transforming GMD maps and cortical thickness reconstructions into region-specific values using appropriate brain atlases. CAT (Gaser et al. 2023) enables this feature

Note: Significant differences were obtained using Fisher's exact test with p < 0.05(two-tailed).

16/5

13/8

13/8

61/5

28/38

34/32

0.057

0.139

0.459

F.1. Deficits in executive

F.2. Relative sparing of

F.3. Relative sparing of

episodic memory

visuospatial skills

tasks

Abbreviations: bvFTD—behavioral variant of frontotemporal dementia; CB-bvFTD and NoCB-bvFTD—groups of bvFTD with and without CB; CB criminal behavior.

segmentation into different tissue classes was performed using the unified segmentation (Ashburner and Friston 2005) approach followed by refined voxel processing including an adaptive maximum a posteriori (AMAP) segmentation (Rajapakse et al. 1997). Resulting segmentations were processed, applying a partial volume estimation which takes the fractional content for each tissue type per voxel into account (Tohka et al. 2004). Spatial normalization was performed with the standard brain of the Montreal Neurological Institute (MNI) using Geodesic Shooting registration (Ashburner and Friston 2011). Finally, modulated gray matter density (GMD) images were smoothed

of performing a region-specific averaging in order to obtain mean tissue and cortical thickness values for different volume and surface-based atlas maps. For GMD, region-specific gray matter values were computed with the LONI Probabilistic Brain Atlas (LPBA40) (Shattuck et al. 2008), while for cortical thickness, region-based analysis was performed with the Desikan–Killiany atlas (Desikan et al. 2006). Note that averaging within regions was performed in the native space before any spatial normalization.

2.4 | Structural MRI Data Group Analysis

In order to test for significant structural differences between bvFTD with and without CB, statistical analysis was performed across all GMD maps and cortical thickness reconstructions using SPM12 (Friston et al. 2007) with the general linear model (GLM) (Kiebel and Mueller 2015) including a full-factorial design (Glascher and Gitelman 2008) with the factors 'group' (CB-bvFTD vs. NoCB-bvFTD) and 'type' (possible bvFTD vs. probable bvFTD). The model also included age, sex, and total intracranial volume (TIV) as additional nuisance covariates. In addition, a binary nuisance covariate was added for each site to encode the location of the center of the FTLD consortium. After parameter estimation, contrast images were computed for the main effect of the group factor. Resulting statistical parametric maps were processed using a voxel-/vertex-threshold of p < 0.001 with a minimum cluster size of k > 500 voxels and vertices, respectively. To correct for multiple comparisons, significant results were obtained with p < 0.05 using family-wise error (FWE) correction at the cluster level (Friston et al. 1994). To further suppress potential false positive findings, clusters were only reported when their maximum remained significant with p < 0.05 using FWE correction at the peak level (Flandin and Friston 2019; Friston et al. 1994; Worsley et al. 1996). Note that this analysis was performed at the full-brain level correcting for all positive findings across the entire brain.

In addition to the comparison between bvFTD with and without CB, we also performed two further analyses comparing both groups of bvFTD (with and without CB) with HC. Both analyses were implemented with a GLM (Kiebel and Mueller 2015) including a full-factorial design (Glascher and Gitelman 2008) with a group factor representing bvFTD vs. HC. The group of bvFTD was again split according to the 'type' factor (possible bvFTD vs. probable bvFTD). Further, we used the same nuisance covariates as described with the previous analysis (age, sex, TIV, site) and the same statistical procedure obtaining significant group differences with p < 0.05 using FWE correction at the cluster- and peak-level (Flandin and Friston 2019; Friston et al. 1994; Worsley et al. 1996).

To investigate a potential effect of the inter-subject variability of disease severity in bvFTD, voxel- and vertex-wise group analyses were also performed using the clinical dementia rate (CDR) as an additional covariate. In addition, we also used the FTLD-CDR in a separate analysis. In order to assess a potential effect of education in the analysis, all voxel- and vertex-wise group comparisons were performed using an enlarged model with an additional covariate including years of education.

Parallel to the voxel- and vertex-wise analyses, region-based analyses were computed based on averaged GMD and cortical thickness values using the CAT (Gaser et al. 2023) toolbox in combination with the LONI (Shattuck et al. 2008) probabilistic brain atlas and the Desikan–Killiany atlas (Desikan et al. 2006), respectively. Here, group differences were investigated between bvFTD with and without CB using the same model as described above. In addition, we also compared both groups of bvFTD (with and without CB) with HC. All analyses were performed with the CAT toolbox using the SPM.mat file generated from the voxel–/vertex-wise analyses. Significant group differences were obtained correcting for multiple comparisons using a false discovery rate (FDR) of 0.05 (Chumbley et al. 2010; Chumbley and Friston 2009).

In addition to the group analyses comparing bvFTD patients with and without CB, that is, analyses within patients showing bvFTD, we performed further group analyses comparing patients with bvFTD with our other cohorts obtained from the data of the FTLD consortium (see subsection 2.2). Voxel-/ vertex-wise and region-based analyses were performed comparing patients showing RATL predominance (RATL-FTD) with CB-bvFTD, NoCB-bvFTD, and HC. In addition, we also compared our svPPA cohort with all three groups CB-bvFTD, NoCB-bvFTD, and HC. In contrast to the models above, statistical analyses were performed using two-sample t-tests including age, sex, and TIV as additional nuisance covariates. Significant group differences were analyzed with the same thresholds as described above, that is, with p < 0.05 using FWE correction at the cluster- and peak-level (Flandin and Friston 2019; Friston et al. 1994; Worsley et al. 1996) for the voxel- and vertex-wise analyses, and using an FDR of 0.05 with the region-based analyses (Chumbley et al. 2010; Chumbley and Friston 2009).

2.5 | Structural MRI and Behavioral Data Correlation Analysis

Complementary to the group analyses described above, we also investigated a potential relationship between brain structure and behavioral impairment using the FrSBe values for frequency and distress of all three behavioral categories: executive dysfunction, disinhibition, and apathy (Grace and Malloy 2020; Stout et al. 2003). Analysis was performed using SPM12 (Friston et al. 2007) with a GLM (Kiebel and Mueller 2015) using a twosample t-test to implement a group factor separating bvFTD with and without CB. In addition, a covariate was used to include the FrSBe values (Grace and Malloy 2020) which were implemented to encode an interaction with the group factor represented by two columns in the design matrix for each group of bvFTD, including patients with and without CB. FrSBe values were demeaned with the group factor, that is, for each group separately. Further columns were added for other nuisance covariates, such as age, sex, and TIV. Finally, contrast images were generated to investigate a potential correlation between brain structure (GMD and cortical thickness) and FrSBe values within the whole group of bvFTD and within both subgroups of bvFTD with and without CB separately. In addition, contrasts were used to model the interaction between the FrSBe covariate and the group factor in order to investigate a potential group difference between bvFTD with and without CB with respect to the correlation between brain structure and all FrSBe subscales. To detect significant results, the same statistical approach was used as with the voxel-/vertex-wise group analyses using a threshold of p < 0.05,

including FWE correction at the voxel- and peak-level (Flandin and Friston 2019; Friston et al. 1994; Worsley et al. 1996).

Potential correlations between brain structure and FrSBe values were also investigated with region-based analyses using the same procedure as implemented with the group analysis using the CAT (Gaser et al. 2023) toolbox with the SPM.mat file. In particular, we investigated a potential correlation between brain structure (GMD and cortical thickness) and behavioral outcome using the FrSBe values in both groups of bvFTD with and without CB separately, and a potential group difference with respect to this correlation. We also investigated a potential correlation across the whole group including all patients with bvFTD. Significant correlations and group differences were obtained correcting for multiple comparisons using an FDR of 0.05 (Chumbley et al. 2010; Chumbley and Friston 2009).

2.6 | Functional MRI Data Pre-Processing

Functional MRI data were obtained using gradient-echo echo planar imaging (EPI) (Mansfield et al. 1994; Stehling et al. 1991) using a repetition time of 2s, and an in-plane resolution of 3 mm with an image matrix of 64×64 pixels. A set of 300 functional volumes was obtained resulting in a scanning duration of 10 min. A reduced number of volumes was obtained for a small number of 4 and 8 patients with and without CB, respectively, which was taken into account within the statistical analysis implementing a nuisance covariate including the number of functional volumes. Image acquisition was performed in the so-called 'resting-state' (Biswal et al. 1995). That is, participants were instructed to remain still and awake, but they had no specific cognitive task to perform. All functional MRI data sets were processed with the CONN toolbox (Whitfield-Gabrieli and Nieto-Castanon 2012) rev. 22a (Nieto-Castanon and Whitfield-Gabrieli 2022) and SPM12 (Friston et al. 2007) rev. 7771 with MATLAB 9.13 rev. 2022b (The MathWorks Inc.). Pre-processing was performed using the default pipeline (Nieto-Castanon 2020b) including realignment with correction of susceptibility distortion interactions, outlier detection, direct segmentation, MNI-space normalization, and smoothing. Functional data were realigned using the SPM realign & unwarp procedure (Andersson et al. 2001), where all scans were co-registered to a reference image (first scan of the first session) using a least squares approach and a six-parameter rigid body transformation (Friston et al. 1995), and resampled using b-spline interpolation to correct for motion and magnetic susceptibility interactions. Potential outlier scans were identified using ART (Whitfield-Gabrieli et al. 2011) according to framewise displacement and global signal changes (Nieto-Castanon 2022; Power et al. 2014), and a reference image was computed for each subject by averaging all scans excluding outliers. Functional and anatomical data were normalized into standard MNI space, segmented into gray matter, white matter, and cerebrospinal fluid (CSF) tissue classes, and resampled to 2 mm isotropic voxels following a direct normalization procedure (Calhoun et al. 2017; Nieto-Castanon 2022) using the SPM unified segmentation and normalization algorithm (Ashburner 2007; Ashburner and Friston 2005) with the default IXI-549 tissue probability map template. Finally, functional data were smoothed using spatial convolution with a Gaussian kernel of 8mm FWHM. Image pre-processing also included denoising within the CONN

toolbox (Nieto-Castanon and Whitfield-Gabrieli 2022; Whitfield-Gabrieli and Nieto-Castanon 2012) using CONN's standard denoising pipeline (Nieto-Castanon 2020a) including the regression of potential confounding effects characterized by signals of white matter and CSF, where no 'true' brain activation should be located, obtained by the CompCor (Behzadi et al. 2007) approach. CompCor noise components within white matter and CSF were estimated by computing the average signal as well as the largest principal components orthogonal to the average, motion parameters, and outlier scans within each subject's eroded segmentation masks (Behzadi et al. 2007; Chai et al. 2012). In addition, nuisance regression also included the translational and rotational parameters from head movements including firstorder derivatives and quadratic effects (also called the Friston-24 model) (Friston et al. 1996), scrubbing covariates using the default CONN settings based on framewise displacement and signal change attributed to head motion (Power et al. 2014), and the effect of the beginning of the resting-state measurement (two regressors). Pre-processing was finalized using detrending and despiking, and band-pass filtering with the default cut-off frequencies of 0.008 and 0.09 Hz (Hallquist et al. 2013).

2.7 | Functional MRI Data Analysis

Using the pre-processed functional MRI data, seed-based connectivity analysis was performed using the CONN toolbox (Whitfield-Gabrieli and Nieto-Castanon 2012) computing seedto-voxel correlations for all voxels across the entire brain. Seed regions were obtained from the analysis showing structural differences between bvFTD with and without CB, and for regions of the left and right temporal lobes using CONN's brain parcellation based on the Harvard-Oxford atlas (Desikan et al. 2006). Functional connectivity strength was represented by Fishertransformed bivariate correlation coefficients from a weighted GLM (Nieto-Castanon 2020c), estimated separately for each seed area and target voxel, modeling the association between their signal timeseries. In order to compensate for possible transient magnetization effects at the beginning of each run, individual scans were weighted by a step function convolved with an SPM canonical hemodynamic response function and rectified.

Using the seed regions, seed-based correlation maps were obtained for each participant, which were further processed by subsequent statistical analysis using SPM12 (Friston et al. 2007). The design matrix was created in the same way as used with analyzing group differences with the structural MRI data with a GLM (Kiebel and Mueller 2015) implementing a flexible-factorial design (Glascher and Gitelman 2008) with the factors 'group' (CB-bvFTD vs. NoCB-bvFTD) and 'type' (possible bvFTD vs. probable bvFTD). The model also included age, sex, and the total number of functional volumes as additional nuisance covariates, and in addition, a binary nuisance covariate was added for each site to encode the location of the center of the FTLD consortium. After parameter estimation, contrast images were generated to investigate potential group differences, and statistical parametric maps were processed using a voxel threshold of p < 0.001 with a minimum cluster size of k > 200 voxels. To correct for multiple comparisons, significant results were obtained with p < 0.05 using FWE correction at the cluster level (Flandin and Friston 2019; Friston et al. 1994; Worsley et al. 1996).

In order to assess a potential effect of education in the analysis, we performed the statistical model with and without a covariate containing years of education. Other validation analyses were aimed at accounting for gray matter loss using additional covariates, including region-specific GMD values of each participant.

2.8 | Visualization

Statistical results were exported with SPM12 (Friston et al. 2007) saving the thresholded statistical parametric maps as NIfTI images. Figures showing orthogonal brain slices were generated using the Mango software (Research Imaging Institute, University of Texas Health Science Center) with the 'Build Surface' option and the 'Cut Plane' feature. Figures showing brain surface representations were obtained using the 'Surface Overlay' of the CAT (Gaser et al. 2023) toolbox and the FsAverage template (Fischl et al. 1999).

3 | Results

3.1 | Criminal Behavior in bvFTD Is Associated With More Disinhibition and Less Apathy

As illustrated in Tables 1 and 2, patients with bvFTD and CB showed better verbal fluency, more disinhibition, in particular socially inappropriate behavior and impulsive, rash, or careless actions, and less apathy than patients with bvFTD, but without CB. There were no differences for age, education, disease duration, and severity of dementia as assessed with MMSE, CDR, FTLD-CDR, or impairments of daily living between both bvFTD groups. Furthermore, there were no differences in the other cognitive measures (Table 1) and behavioral alterations (Table 2) between both bvFTD groups. As expected, patients with bvFTD generally were impaired in these cognitive and clinical measures compared with healthy controls.

3.2 | Criminal Behavior in bvFTD Is Related to Reduced Gray Matter Density in the Temporal Lobe

The VBM analysis comparing structural MR images between bvFTD with and without CB (CB-bvFTD vs. NoCB-bvFTD) showed a significant GMD decrease with CB in the left temporal lobe predominantly in the vicinity of the hippocampus but also other anterior regions within the left temporal lobe (Figure 2A). Including CDR or FTLD-CDR as a confounding covariate showed a nearly identical result (Figure S1, left panel). No other cluster was detected within this comparison. The inverse contrast of a potential GMD increase with CB did not show any significant result. Comparing CB-bvFTD with HC, a GMD decrease was obtained with CB in the left and the right temporal lobe with maximum values in the left hemisphere (Figure 2B), which is in line with the comparison within bvFTD with and without CB (see Figure 2A). The inverse contrast investigating a potential GMD increase with CB, compared with HC, did not reveal any significant result. We also compared NoCB-bvFTD with HC and obtained a significant GMD decrease with bvFTD in wide cortical regions of the frontal and temporal lobe without any signs of asymmetry between GMD decrease in the left

and right hemisphere (Figure 2C). The inverse contrast related to a GMD increase with bvFTD, compared with HC, did not show any significant result. Note that including years of education as an additional covariate showed nearly identical results (Figure S2).

In addition to the GMD-related voxel-based analysis, we also performed a region-based analysis using the LONI (Shattuck et al. 2008) probabilistic brain atlas. Results were in line with the voxel-based analysis showing reduced GMD in the left temporal lobe when comparing bvFTD with and without CB, including the left hippocampus (Figure 2D). The comparison between CB-bvFTD and HC revealed GMD decline in widely distributed regions of the frontal and temporal lobe, including maximum values in the left temporal lobe (Figure 2E). Comparing between NoCB-bvFTD and HC, GMD diminishment showed an even more prominent pattern across the entire brain, most prominently in the frontal and temporal lobe (Figure 2F). Note that we also computed the inverse contrast related to a GMD increase with CB with the comparisons between bvFTD with and without CB, and between CB-bvFTD and HC. However, we did not find any significant GMD increase related to CB. The inverse contrast for the third contrast comparing NoCB-bvFTD and HC did not show any significant GMD increase with bvFTD.

3.3 | Criminal Behavior in bvFTD Is Related to Reduced Cortical Thickness in the Temporal Lobe

Results of vertex-wise cortical thickness analyses were in line with the results obtained with GMD, showing a diminishment of brain structure in the same brain regions. Comparing bvFTD with and without CB (CB-bvFTD vs. NoCB-bvFTD), we obtained significantly decreased cortical thickness with CB in the left temporal lobe, predominantly in anterior regions including the left temporal pole (Figure 3A). Including CDR or FTLD-CDR as a confounding covariate showed a nearly identical result (Figure S1, right panel). Decreased cortical thickness was also observed in the left temporal lobe when comparing between CB-bvFTD and HC (Figure 3B). Reduced cortical thickness was obtained with CB in both the left and the right temporal lobe; however, more dominantly in the left hemisphere, which is in line with the contrast comparing bvFTD with and without CB (compare Figure 3A,B). Interestingly, when comparing between NoCB-bvFTD and HC, diminished cortical thickness was mainly observed in the frontal lobe and less pronounced in temporal regions (Figure 3C). The inverse contrasts looking for a potential increase in cortical thickness with CB (comparing between CB-bvFTD and NoCB-bvFTD, and comparing between CB-bvFTD and HC) did not reveal any significant result. We also did not find any significant increase in cortical thickness when comparing between NoCB-bvFTD and HC. Note that including years of education as an additional covariate showed nearly identical results (Figure S3).

The region-based analysis (Gaser et al. 2023) and the Desikan-Killiany atlas (Desikan et al. 2006) showed a significant decrease in cortical thickness with CB in line with the results of the vertex-wise analysis. Comparing bvFTD with and without CB (CB-bvFTD vs. NoCB-bvFTD), we obtained a significant decrease in the left temporal lobe predominantly in anterior

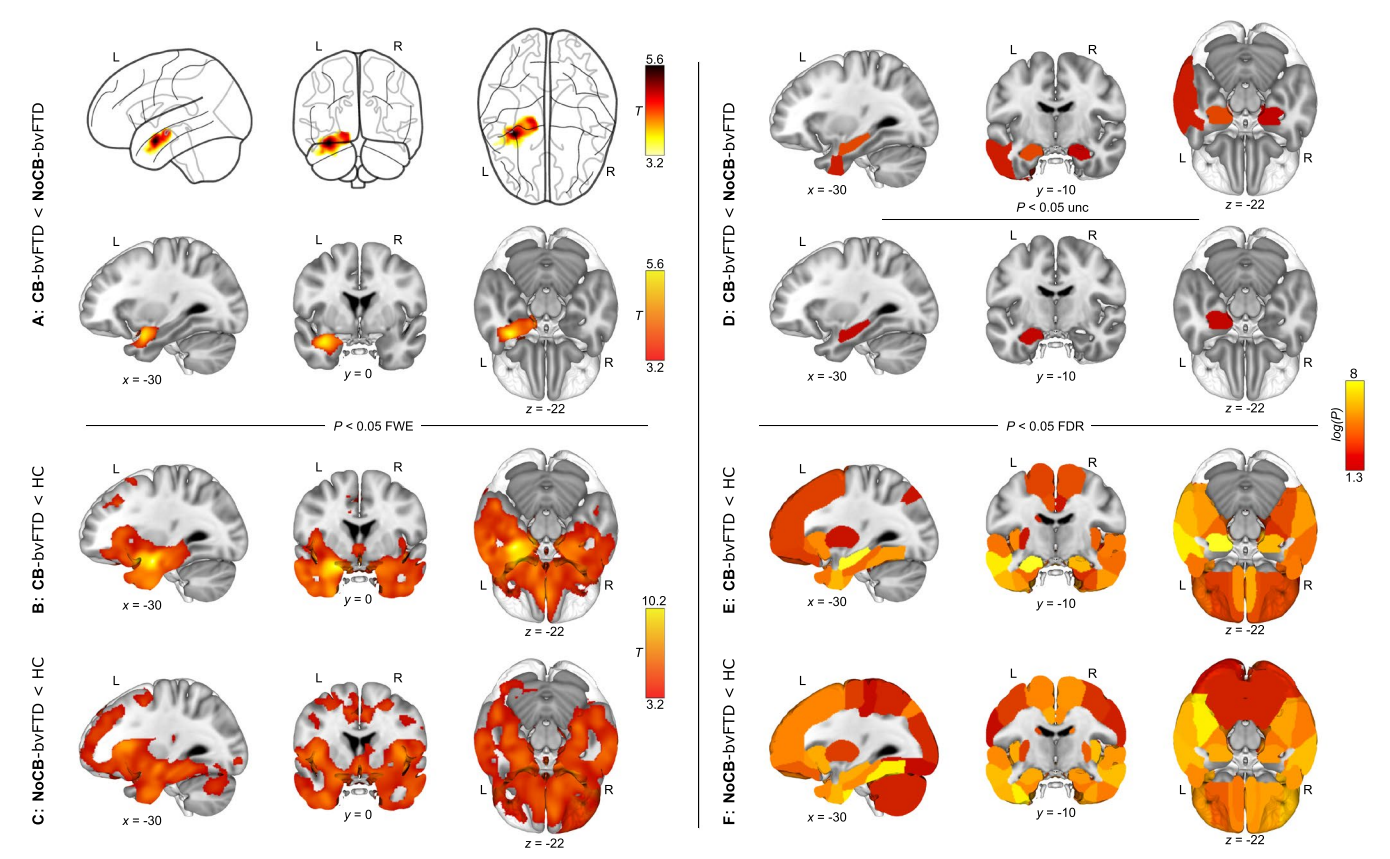


FIGURE 2 | Voxel-based analysis (left panel) and region-based analysis (right panel) showing gray matter density (GMD) decrease with criminal behavior in the behavioral variant of frontotemporal dementia (bvFTD). (A, D) Comparing bvFTD with and without criminal behavior (CB-bvFTD vs. NoCB-bvFTD), a significant GMD decrease was obtained with criminal behavior in the left temporal lobe including left hippocampus. (B, E) Comparing CB-bvFTD with healthy controls (HC), GMD decrease was observed in widely distributed regions of the temporal and frontal lobe with the maximum decrease in the left temporal lobe. (C, F) Comparing NoCB-bvFTD with HC, GMD decrease was obtained in the left and the right temporal lobe. Significant results were obtained with p < 0.05 using family-wise error (FWE) correction for voxel-based analysis (left panel) and false discovery rate (FDR) for the region-based analysis (right panel). L—left, R—right, unc—uncorrected, x, y, z—coordinates in mm.

regions including the left temporal pole (Figure 3D). In contrast to the vertex-wise analysis, we also obtained a significant cortical thickness decrease in the right temporal pole (compare Figure 3A,D). The comparison between CB-bvFTD and HC revealed diminished cortical thickness with CB in the frontal and temporal lobes with maximum differences in the left and right temporal lobes (Figure 3E). The comparison between NoCB-bvFTD and HC showed a significant cortical thickness decrease in widely distributed cortical regions; however, with maximum values in the frontal lobe and not in regions of the temporal lobe (Figure 3F). All inverse contrasts looking for a potential cortical thickness increase with CB did not show any significant results. We also did not find any significant result when investigating a potential cortical thickness increase with bvFTD when comparing bvFTD with HC.

3.4 | Brain Structure Alterations Are Distinct in bvFTD With Criminal Behavior and RATL-FTD and svPPA

The statistical comparison between GMD of RATL-FTD and CB-bvFTD revealed significant GMD differences in regions of the right temporal lobe showing lower GMD values with the RATL-FTD group (see Figure 4A for the voxel-based analysis,

and Figure 4D for the region-based analysis). No result was obtained in the left temporal lobe. The same finding was obtained by investigating cortical thickness showing lower values with the RATL-FTD group in the right temporal lobe but not in the left temporal lobe (see Figure 5A,D for the vertexand region-based analysis, respectively). In contrast, other group comparisons investigating GMD and cortical thickness differences between RATL-FTD and NoCB-bvFTD and between RATL-FTD and HC showed a significant decrease with the RATL-FTD group bilaterally, but still more pronounced in the right temporal lobe (see panels B, C, E, and F of Figures 4 and 5).

The inverse contrast investigating a reduced GMD and cortical thickness with CB-bvFTD, compared with RATL-FTD, did not show any significant results, neither on the voxel—/vertex-level nor with the region-based analysis.

The statistical comparison between GMD of svPPA and CB-bvFTD showed significant GMD differences in both the left and the right temporal lobes but predominantly in the left hemisphere, showing smaller GMD values with the svPPA group (see Figure 6A for the voxel-based analysis, and Figure 6D for the region-based analysis). The same finding was obtained by investigating cortical thickness, showing lower values with the svPPA

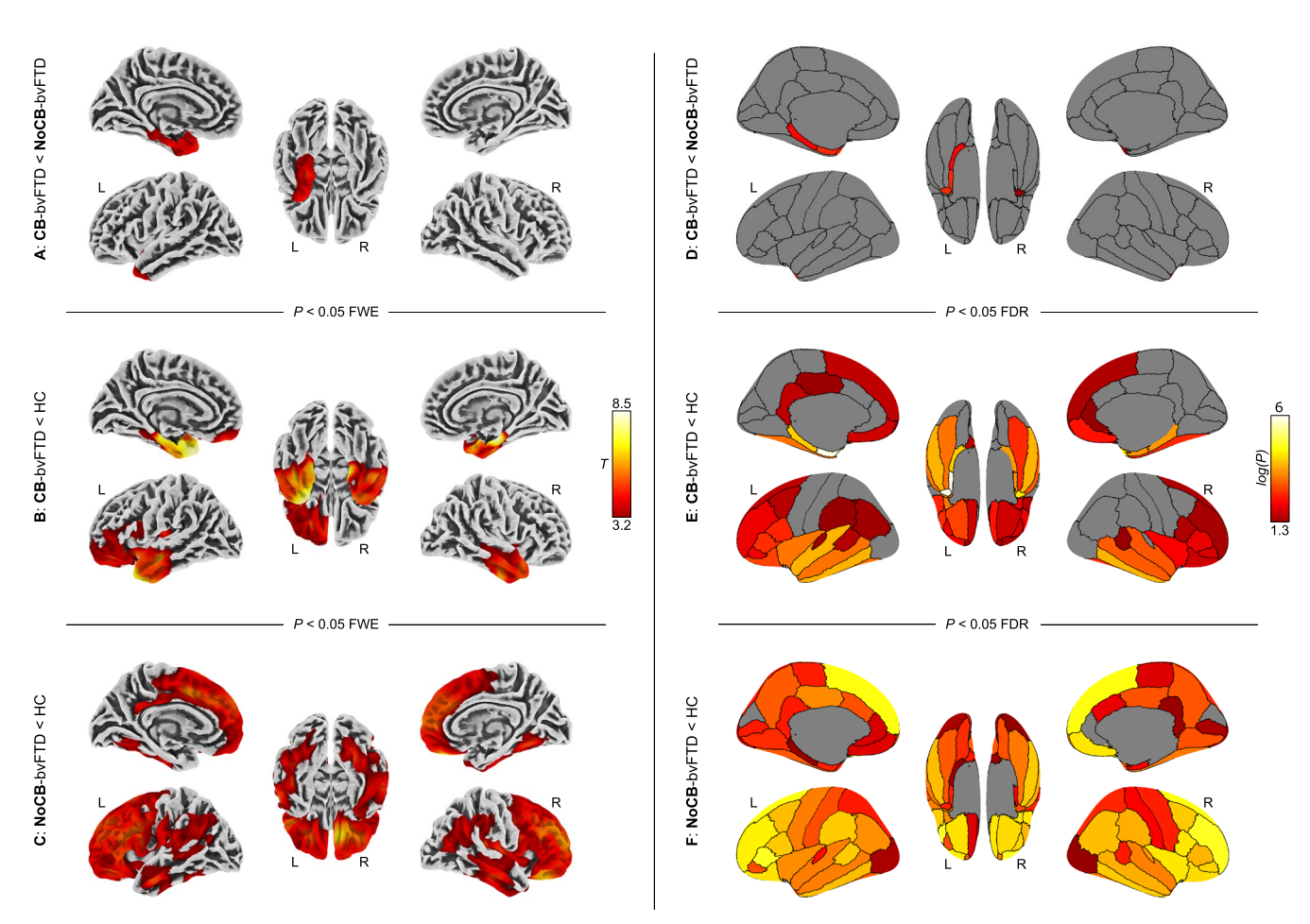


FIGURE 3 | Vertex-based analysis (left panel) and region-based analysis (right panel) showing decreased cortical thickness with criminal behavior in the behavioral variant of frontotemporal dementia (bvFTD). (A, D) Comparing bvFTD with and without criminal behavior (CB-bvFTD vs. NoCB-bvFTD), a significant decrease of cortical thickness was obtained with criminal behavior in the left temporal lobe. (B, E) Comparing CB-bvFTD with healthy controls (HC), cortical thickness decrease was obtained in widely distributed regions of the left and right temporal lobe including regions of the frontal lobe. (C, F) Comparing NoCB-bvFTD with HC, cortical thickness decrease was obtained in the left and the right hemisphere predominantly in the frontal lobe. Significant clusters were obtained with p < 0.05 using family-wise error (FWE) correction for vertex-based analysis (left panel) and false discovery rate (FDR) for the region-based analysis (right panel). L—left, R—right.

group in the left (and the right) temporal lobes (see Figure 7A,D for the vertex- and region-based analysis, respectively). Interestingly, the same result was obtained when comparing the svPPA group with NoCB-bvFTD and with HC, showing reduced GMD and cortical thickness with svPPA in the left and right temporal lobes but predominantly in the left temporal lobe (see panels B, C, E, and F of Figures 6 and 7).

The inverse contrast investigating a reduced GMD and cortical thickness with CB-bvFTD, compared with svPPA, did not show any significant result, neither on the voxel- nor on the vertex level. In the region-based analysis, we obtained a marginal result showing a reduced cortical thickness with CB-bvFTD in regions of the inferior frontal gyrus (not shown).

3.5 | Disinhibition Is Related to Reduced Gray Matter Density in the Temporal Lobe Specifically in bvFTD With Criminal Behavior

As mentioned before in Section 3.1, CB was associated with more disinhibition and less apathy in bvFTD on a clinical

level. To investigate the relationship between brain structure and behavioral impairment in bvFTD with and without CB, we investigated a potential correlation between GMD and all six FrSBe (Grace and Malloy 2020) covariates (frequency and distress of all three behavioral categories: executive dysfunction, disinhibition, and apathy). However, using a voxel-based analysis, we did not find any significant positive or negative correlation between GMD and all six FrSBe subscales, neither across the whole group of bvFTD nor for the subgroups of bvFTD with and without CB. We also did not find any significant interaction between any of the FrSBe subscales and the group factor.

In contrast to absent results at the voxel level, the region-based analysis revealed a significant negative correlation between GMD and two FrSBe subscales: frequency of apathy and distress of disinhibition. Across all patients with bvFTD, we found a significant negative correlation between GMD and frequency of apathy in putamen and caudate bilaterally. This correlation also became significant within the subgroup of bvFTD showing CB, and for the right putamen, we even obtained a significant interaction between this correlation and the group factor, showing a

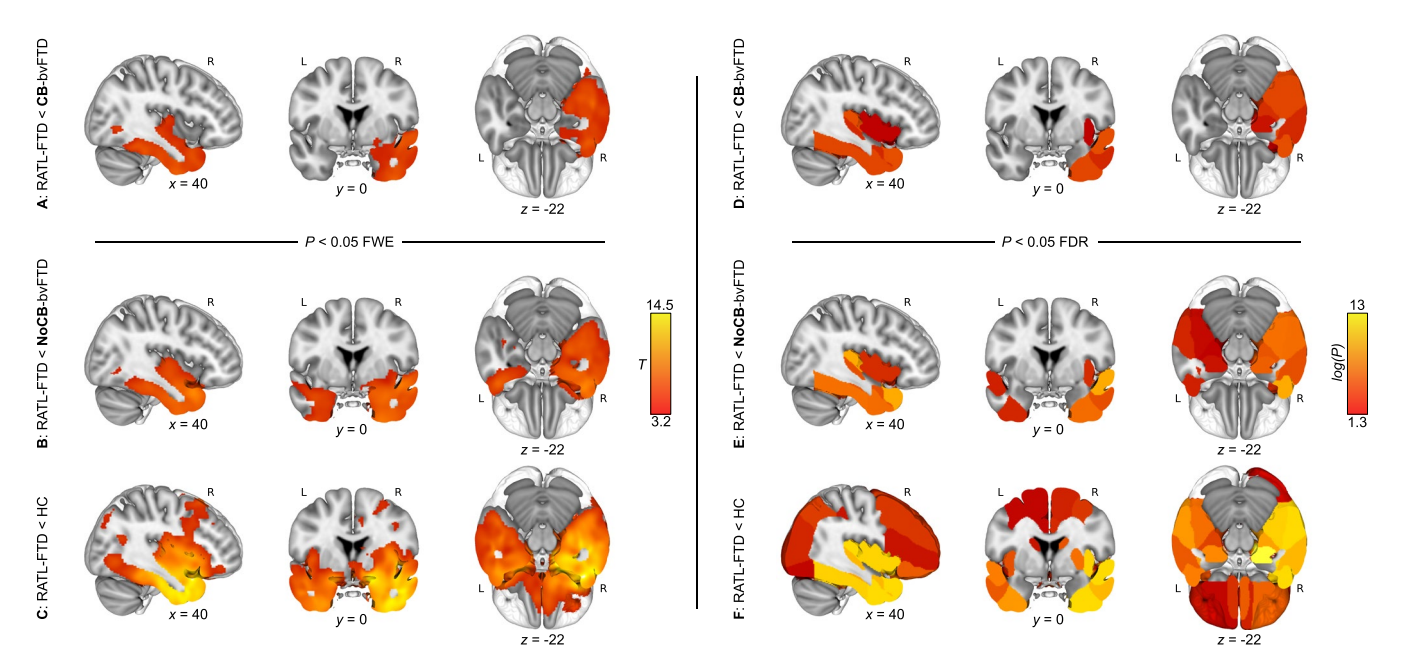


FIGURE 4 | Voxel-based analysis (left panel) and region-based analysis (right panel) presenting decreased gray matter density (GMD) in patients with frontotemporal dementia (FTD) showing right anterior temporal lobe predominance (RATL-FTD) compared with (A, D) patients showing criminal behavior in the behavioral variant of FTD (CB-bvFTD), (B, E) patients with bvFTD showing no criminal behavior (NoCB-bvFTD), and (C, F) healthy controls (HC). Significant results were obtained with p < 0.05 using family-wise error (FWE) correction for the voxel-based analysis (left panel) and false discovery rate (FDR) for the region-based analysis (right panel). L—left, R—right, x, y, z—coordinates in mm.

significant group difference between patients with and without CB with respect to the correlation between GMD and frequency of apathy (not shown).

Across all patients with bvFTD (All-bvFTD), we also obtained a significant negative correlation between GMD and distress of disinhibition in the left superior temporal gyrus (STG) (Figure 8A). This negative correlation became even more prominent within the subgroup of patients showing CB (CB-bvFTD, Figure 8B). The maximum negative correlation was obtained in the left STG. A significant negative correlation between GMD and distress of disinhibition was obtained in further brain regions within the left temporal lobe, but also in the precentral gyrus, fusiform gyrus, hippocampus, and putamen (see Figure 8B). Interestingly, we did not observe any significant negative or positive correlation between GMD and distress of disinhibition within the subgroup of patients without signs of CB (NoCB-bvFTD, see Figure 8C). Finally, the interaction between the group factor and distress of disinhibition revealed a significant group difference between bvFTD with and without CB with respect to the correlation between GMD and distress of disinhibition. This significant result was obtained in many brain regions, including the left temporal lobe, the frontal lobe, but also subcortical brain regions including the putamen and caudate bilaterally (Figure 8D).

3.6 | Disinhibition Is Related to Reduced Cortical Thickness in the Temporal Lobe—Specifically in bvFTD With Criminal Behavior

Investigating the relationship between cortical thickness and behavioral impairment of bvFTD with and without CB, we performed a correlation analysis using all six FrSBe covariates implementing frequency and distress of the three behavioral categories. In line with our findings of the region-based GMD analysis (see Figure 8), we obtained a relationship between cortical thickness and distress of disinhibition. Using a vertex-wise analysis, we found a significant negative correlation between distress of disinhibition and cortical thickness in the left anterior STG specifically in CB-bvFTD (Figure 9A). This correlation was not obtained for the subgroup of NoCB-bvFTD (see Figure 9B). The interaction analysis (between the group factor and the FrSBe values) showed a significant group difference between bvFTD with and without CB (Figure 9C), that is, the negative correlation between cortical thickness and distress of disinhibition occurred specifically in bvFTD showing CB.

Note that distress of disinhibition was the only FrSBe covariate showing a significant correlation with cortical thickness on the vertex-level within the bvFTD subgroups, that is, we did not find any other positive or negative correlation on the vertex-level, neither for CB-bvFTD nor within the subgroup of NoCB-bvFTD. We also did not find any significant interaction between any other FrSBe covariate and the group factor.

In line with the vertex-wise analysis, the region-based analysis (Gaser et al. 2023) using the Desikan–Killiany atlas (Desikan et al. 2006) showed a significant negative correlation between cortical thickness and distress of disinhibition, particularly in bvFTD with CB predominantly in the left temporal lobe showing maximum values in the left STG (Figure 9D). This negative correlation was also obtained in other cortical regions, including areas within the frontal and parietal lobes. In contrast, no significant correlation was obtained for the subgroup

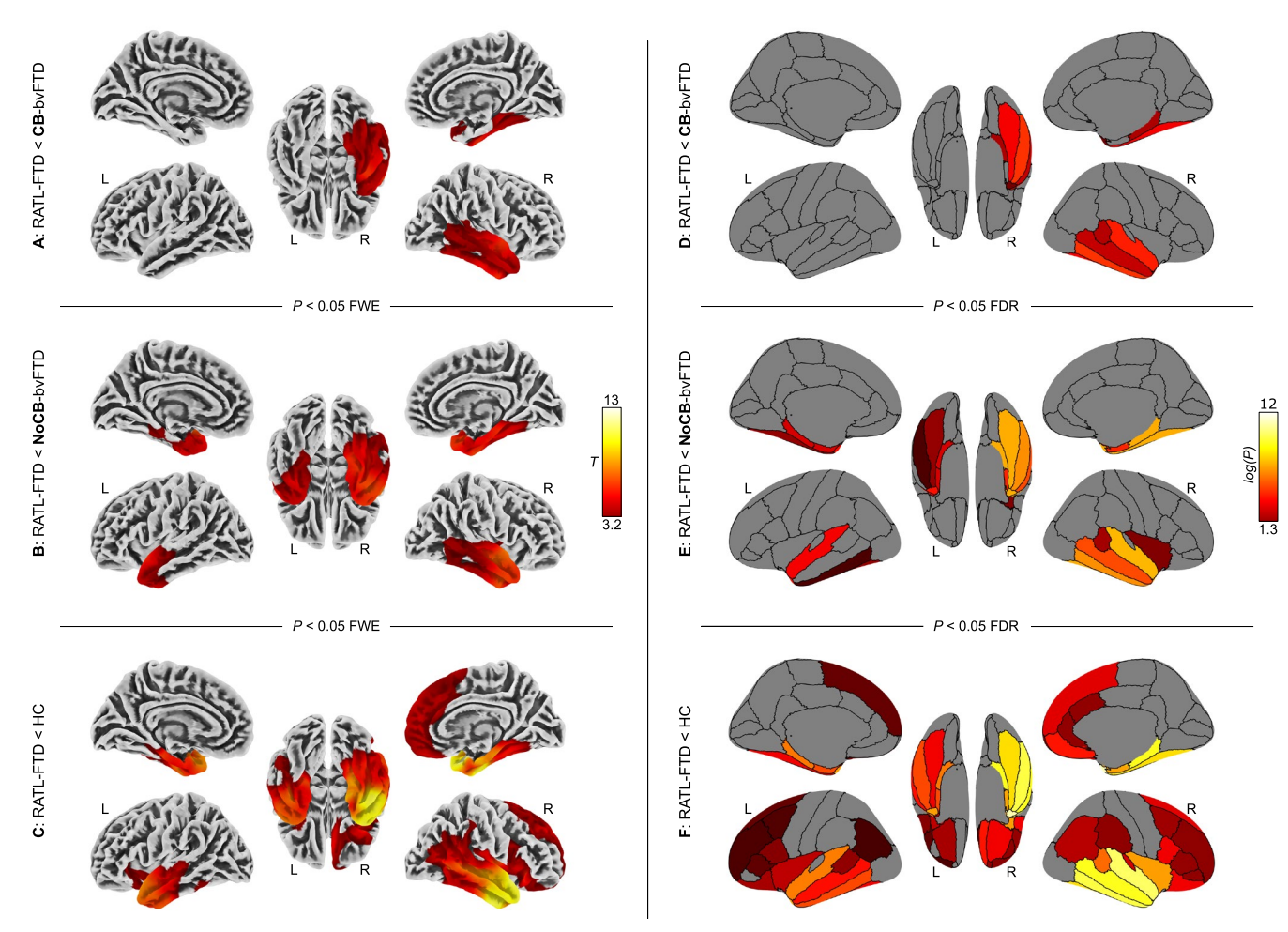


FIGURE 5 | Vertex-based analysis (left panel) and region-based analysis (right panel) presenting decreased cortical thickness in patients with frontotemporal dementia (FTD) showing right anterior temporal lobe predominance (RATL-FTD) compared with (A, D) patients showing criminal behavior in the behavioral variant of FTD (CB-bvFTD), (B, E) patients with bvFTD showing no criminal behavior (NoCB-bvFTD), and (C, F) healthy controls (HC). Significant results were obtained with p < 0.05 using family-wise error (FWE) correction for the vertex-based analysis (left panel) and false discovery rate (FDR) for the region-based analysis (right panel). L—left, R—right.

of NoCB-bvFTD, neither positive nor negative (Figure 9E). The group difference (between bvFTD with and without CB) showed a significant interaction between the group factor and the FrSBe subscale of distress of disinhibition (Figure 9F) that demonstrates that the negative correlation is specifically present in bvFTD showing CB.

Apart from the FrSBe subscale of distress of disinhibition, the region-based analysis showed a negative correlation between the frequency of disinhibition and cortical thickness in the left temporal lobe, particularly in the left inferior temporal gyrus, specifically in bvFTD with CB and not in patients without CB (not shown). Note that this result was obtained near the threshold ($p\!=\!0.046$ FDR) including a significant group difference with the interaction analysis. We also found a negative correlation between the frequency of executive dysfunction and cortical thickness in CB-bvFTD; however, we did not obtain a significant interaction between the group factor and the FrSBe subscale, that is, we did not obtain a significant group difference between bvFTD with and without CB.

3.7 | Criminal Behavior in bvFTD Is Related to Reduced Functional Connectivity Between the Temporal Lobe and Frontoparietal Brain Regions

Based on our findings using the structural MRI data, revealing the left temporal lobe as the most prominent hub for CB in bvFTD, we performed seed-based connectivity analyses with various seed regions using the VBM result and areas of the left temporal lobe available with CONN's brain parcellation as the left planum polare (PP), the left anterior STG, the left temporal pole (TP), and the anterior part of the left parahippocampal cortex (PaHC). To show the specificity of the results using seed regions within the left temporal lobe, we also investigated the same seed regions within the right temporal lobe, that is, the right PP, the right anterior STG, the right TP, and the anterior part of the right PaHC.

Using a seed mask based on the VBM result (see Figure 2A), we obtained significant functional brain connectivity differences between bvFTD with and without CB. We obtained a significant decrease of seed-based connectivity with CB

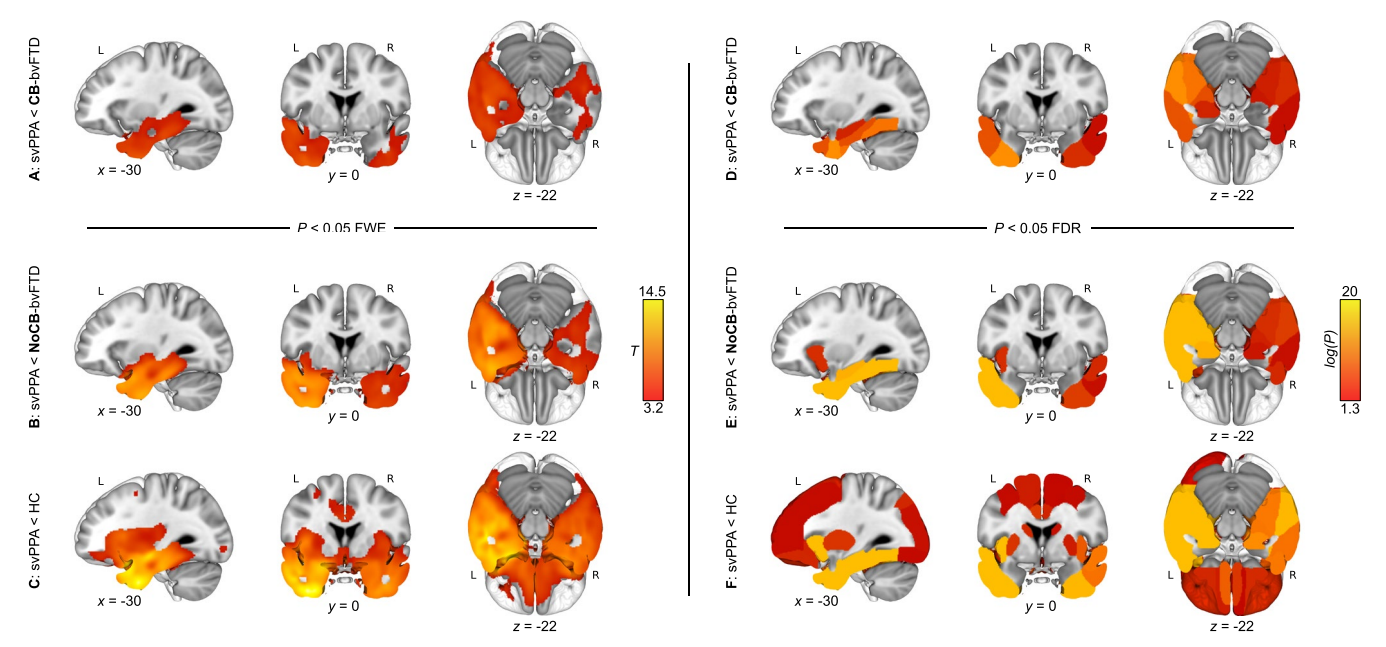


FIGURE 6 | Voxel-based analysis (left panel) and region-based analysis (right panel) showing decreased gray matter density (GMD) in patients with the semantic variant of primary progressive aphasia (svPPA) compared with (A, D) patients showing criminal behavior in the behavioral variant of FTD (CB-bvFTD), (B, E) patients with bvFTD showing no criminal behavior (NoCB-bvFTD), and (C, F) healthy controls (HC). Significant results were obtained with p < 0.05 using family-wise error (FWE) correction for the voxel-based analysis (left panel) and false discovery rate (FDR) for the region-based analysis (right panel). L—left, R—right, x, y, z—coordinates in mm.

between the region of the VBM result within the left temporal lobe (Figure 10A, blue color) and regions of the default mode network in the posterior cingulate cortex (PCC) and the right temporoparietal junction (TPJ) (Figure 10A, red color). This group difference was also obtained for the left TPJ when using the analysis without correction for multiple comparisons. Note that no seed-based connectivity increase was observed with CB using VBM's seed mask.

Comparing seed-based functional connectivity between bvFTD with and without CB using CONN's atlas in regions of the left temporal lobe, we obtained a connectivity decrease with CB when using the left anterior STG, the left PP, the left TP, and the left anterior PaHC as seed regions. The most prominent group differences were found using seed regions in the left PP and in the left anterior STG (Figure 10B,C, respectively). Specifically, we obtained a significant connectivity decrease between these seed regions and widely distributed cortical areas, particularly with the left and right premotor cortex in the vicinity of the left and right precentral sulcus (Figure 10B,C). Interestingly, for the seed region of the left anterior STG, we also found a significant connectivity decrease with CB between this seed and the left and right inferior frontal junction (IFJ) (Figure 10C,D). Note that we also investigated the inverse contrast looking for a potential brain connectivity increase with CB with all seed regions mentioned above; however, we did not find any significant result.

Using an enlarged model with an additional covariate including years of education, the statistical analysis produced nearly identical results (Figure S4). We also performed a validation analysis in order to account for gray matter loss within the left temporal lobe (see Figure 2A). For each participant, we extracted GMD values (a) for the maximum of the cluster, and (b) within all voxels of the cluster using the first eigenvariate providing a weighted

mean where atypical voxels are down-weighted. These extracted GMD values were further used as additional covariates in the GLM in order to account for the observed region-specific gray matter loss. However, adding the GMD covariates did not show any substantial effect for both approaches using the maximum (Figure S5) or the first eigenvariate (Figure S6).

Comparing seed-based functional connectivity between bvFTD with and without CB using CONN's atlas in specific regions of the right temporal lobe, we obtained no significant results when using the right anterior STG and the right anterior PaHC as seed regions (see Figure 11A,D, respectively). Using the right TP and the right PP, we obtained a functional connectivity decrease with CB, but on a far smaller scale compared with using seed regions within the left temporal lobe (see Figure 11B,C, respectively). In particular, we did not obtain any CB-related functional connectivity alterations between seeds within the right temporal lobe and the IFG as we obtained when using the left anterior STG as the seed region. Note that the inverse contrast looking at a potential CB-related functional connectivity increase did not show any significant result for any seed region within the left and the right temporal lobe.

4 | Discussion

In our study, we investigated potential structural and functional brain alterations with CB, particularly comparing between bvFTD with and without CB, and between bvFTD showing CB with HC. We found a major impairment of CB onto brain structure in the temporal lobe, predominantly in the left hemisphere. In particular, we found a consistent decrease of GMD and cortical thickness with CB using voxel-/vertex-wise and region-based analyses with the LONI (Shattuck et al. 2008) and the Desikan–Killiany

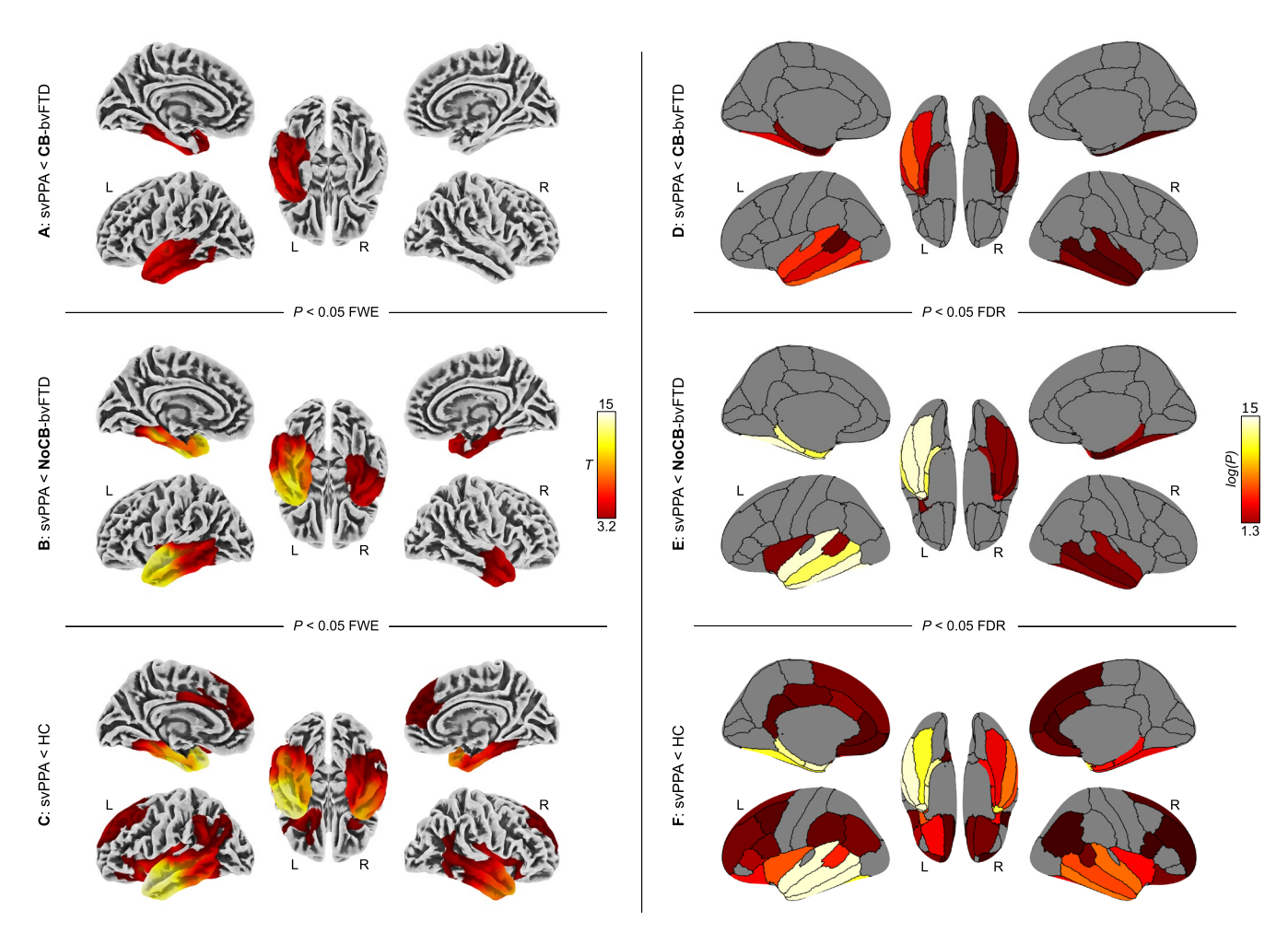


FIGURE 7 | Vertex-based analysis (left panel) and region-based analysis (right panel) showing decreased cortical thickness in patients with the semantic variant of primary progressive aphasia (svPPA) compared with (A, D): patients showing criminal behavior in the behavioral variant of FTD (CB-bvFTD), (B, E): patients with bvFTD showing no criminal behavior (NoCB-bvFTD), and (C, F): healthy controls (HC). Significant results were obtained with *p* < 0.05 using family-wise error (FWE) correction for the vertex-based analysis (left panel) and false discovery rate (FDR) for the region-based analysis (right panel). L—left, R—right.

(Desikan et al. 2006) atlas, respectively. These group differences were accompanied by a tight relationship between behavioral impairment scores and brain structure using the FrSBe scale. In bvFTD showing CB, we found a significant correlation between distress of disinhibition and brain structure (GMD as well as cortical thickness) in the same region as obtained with the group differences, namely within the left temporal lobe. This relationship was not found in bvFTD without CB, and we even obtained a significant interaction between distress of disinhibition with the group factor (bvFTD with and without CB) demonstrating a significant group difference with respect to the correlation between disinhibition and brain structure. Notably, CB was associated with higher disinhibition and verbal fluency, and less apathy in bvFTD on a clinical level. Accordingly, disinhibition seems to be the most important driver for CB in our bvFTD cohort.

4.1 | Criminal Behavior Is Related to Temporal Lobe Dysfunction in bvFTD in Interaction With Disinhibition

Our results suggest that CB in bvFTD is related to a major impairment of brain areas within the temporal lobe and adjacent

cortical and subcortical regions, predominantly in the left hemisphere. Although the current literature does not show any findings comparing bvFTD with and without CB using VBM, there are a couple of VBM studies investigating brain structure impairment in persons showing antisocial behavior in psychopathy. In line with our results, studies consistently found an involvement of regions within the temporal lobe: In a study investigating violent offenders with antisocial behavior already emerging in childhood, psychopathy was associated with a major GMD decrease in the left and right temporal lobe in the vicinity of the temporal poles, suggesting long-term structural brain changes (Kolla et al. 2014). In line, investigating psychopathy with 17 forensic male patients showed a reduction of GMD in the left and right temporal lobe, particularly in the left and right STG (Muller et al. 2008). Consistently, further work including 15 persons with elevated psychopathy scores showed GMD reduction in the vicinity of the left and right STG and regions of the prefrontal cortex, suggesting an impairment of a frontotemporal network related to the brain representation of moral behavior (de Oliveira-Souza et al. 2008). In a subsequent study combining VBM with support vector machine classification, the left and right STG were identified as regions containing the most relevant information

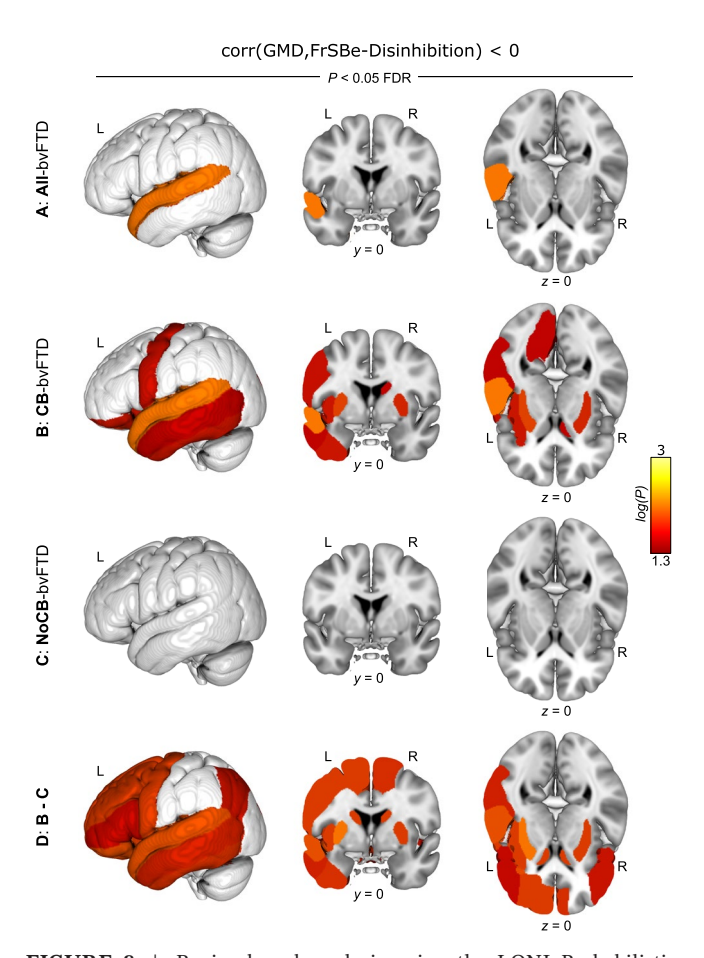


FIGURE 8 | Region-based analysis using the LONI Probabilistic Brain Atlas showing a negative correlation between gray matter density (GMD) and distress of disinhibition obtained with the Frontal Systems Behavioral Scale (FrSBe) in the behavioral variant of frontotemporal dementia (bvFTD). (A) A significant negative correlation between GMD and FrSBe-Disinhibition was obtained across all patients with bvFTD (All-bvFTD) in the left superior temporal gyrus (STG). (B) A negative correlation between GMD and FrSBe-Disinhibition was also obtained in the subgroup of bvFTD showing criminal behavior (CB-bvFTD). The maximum was located in the left STG, but significant correlation was also obtained in other brain regions including regions within the left temporal lobe. (C) Neither negative nor positive correlation was obtained with bvFTD showing no criminal behavior (NoCB-bvFTD). (D) An interaction analysis revealed a significant group difference between bvFTD with and without criminal behavior related to the relationship between GMD and FrSBe-Disinhibition. Significant differences were obtained correcting for multiple comparisons using a false discovery rate (FDR) of 0.05. L—left, R—right, y, z—coordinates in mm.

to classify psychopathy from healthy controls, underlining the major role of the STG for antisocial behavior (Sato et al. 2011). Interestingly, structural decline of the left and right STG with psychopathy was not only found with VBM techniques but also with cortical thickness measures (Ly et al. 2012). Thus, in line with our findings, the literature shows a major agreement about gray matter decline in psychopathy and antisocial behavior specifically in regions of the left and right temporal lobe including the STG.

In addition to the involvement of brain regions with CB within the temporal cortex, we also obtained reduced GMD in regions of the hippocampus and amygdala. While our voxel-based analysis showed its maximum GMD decrease in the left amygdala, the region-based analysis showed the left and right hippocampus as affected by CB. Interestingly, these results are also in line with the current literature on CB in psychopathy showing decreased regional gray matter volume in several paralimbic and limbic areas including bilateral parahippocampal, amygdala, and hippocampal regions (Ermer et al. 2012, 2013). Higher primary psychopathy scores in female judo athletes were negatively associated with gray matter volume in the left amygdala/hippocampus accompanied by anger and lower empathy (Gonzalez-Alemany et al. 2023). In a group of 40 male violent offenders, the risk of recidivism for violence was also negatively correlated with the gray matter volume of the amygdala (Leutgeb et al. 2015). Structural correlates of psychopathy were even found within a sample of healthy adults combining VBM with the Triarchic Psychopathy Measure. Overall psychopathy was negatively correlated with gray matter volume of the left putamen and amygdala, and meanness particularly with amygdala volume (Vieira et al. 2015). In line with our findings, disinhibition was found to be negatively correlated with amygdala volume reflecting a general disposition of impulse control and emotional regulation (Patrick 2008). Our results might be based on similar mechanisms; however, the interaction with FTD needs to be further investigated.

In dementia, CB is commonly aligned with FTD, particularly with bvFTD, and much less frequent with other forms like Alzheimer's disease (Mendez 2022; Mendez, Anderson, and Shapira 2005). This observation is explained by the nature of bvFTD, including its pathophysiological localization associated with a disturbance of social and emotional processing networks constituting various forms of CB (Mendez 2022). In our work, we found the same pattern of atrophy in frontal and temporal brain regions as shown in the literature (Hua et al. 2018) when comparing bvFTD with HC. However, CB in bvFTD was mainly related to GMD and cortical thickness reduction in the left and right temporal lobes. Surprisingly, significant impairment was obtained predominantly in the left hemisphere, suggesting an imbalance between brain degeneration within the left and the right temporal lobes related to CB in bvFTD. Notably, in a recent study including a largely overlapping cohort of the FTLD consortium, such as in our study, Weise and colleagues showed that social cognition deficits in bvFTD, as measured with the Reading the Mind in the Eyes test, were associated with temporal atrophy and not with prefrontal atrophy that was specifically related to executive dysfunction (Weise et al. 2024).

Other studies investigated related behavioral changes in bvFTD. Mychack and colleagues reported that right-sided bvFTD showed more frequently socially undesirable behavior as an initial symptom (including CB) than left-sided bvFTD (Mychack et al. 2001). However, CB was explicitly mentioned for right-sided bvFTD only. In this study, laterality was assessed by MRI and single-photon emission computed tomography (SPECT). Another study by Mendez and colleagues reported that sociopathic acts were associated with right frontotemporal involvement on SPECT/positron emission tomography (PET) in bvFTD (Mendez, Chen, et al. 2005). Another recent work investigated antisocial behavior in a larger cohort including numerous dementia syndromes, where antisocial behavior occurred more

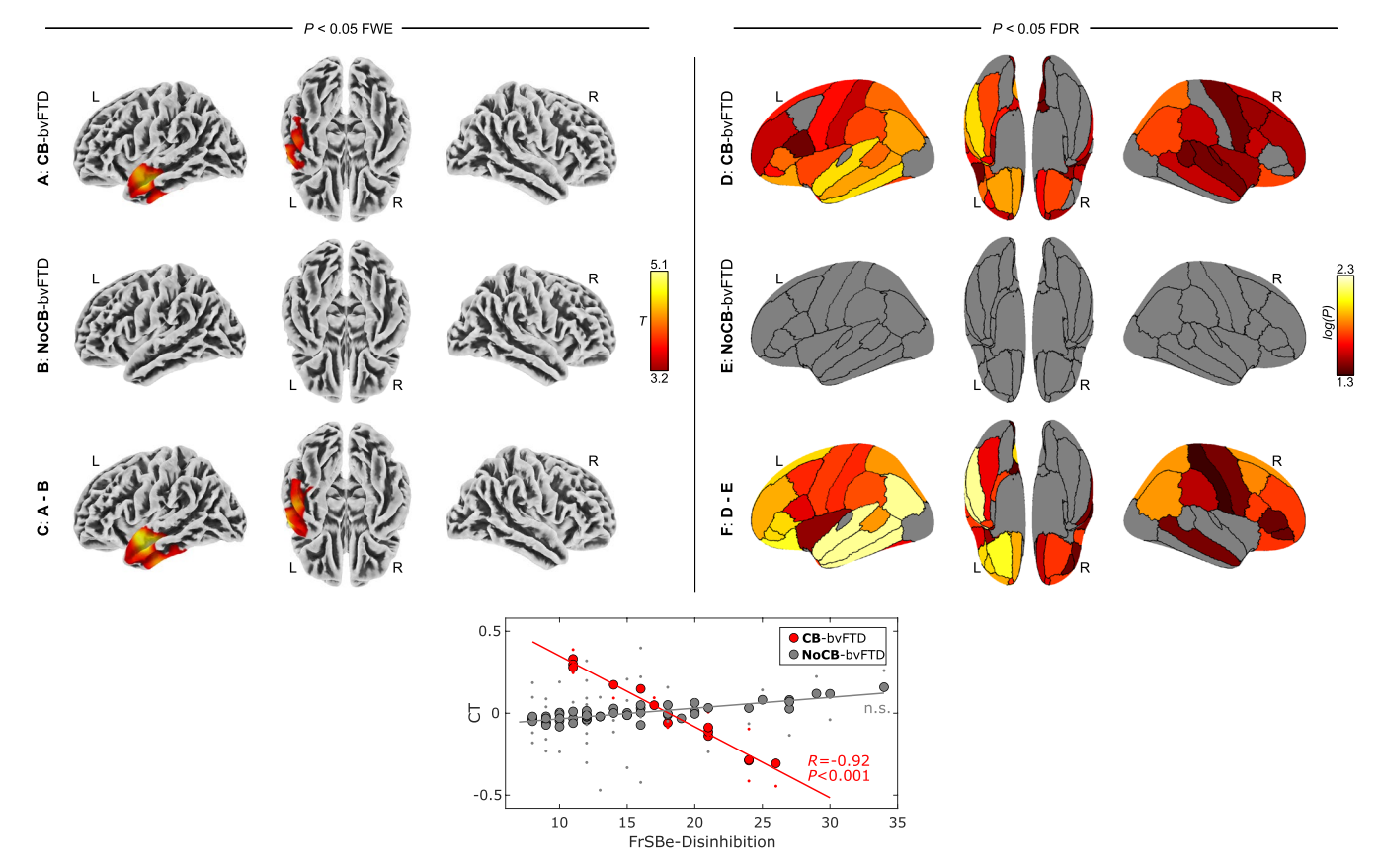
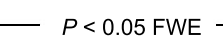


FIGURE 9 | Vertex-based analysis (left panel) and region-based analysis (right panel) showing a negative correlation between cortical thickness (CT) and distress of disinhibition obtained with the Frontal Systems Behavioral Scale (FrSBe) in the behavioral variant of frontotemporal dementia (bvFTD). (A, D) A significant negative correlation between CT and FrSBe-Disinhibition was obtained with patients showing criminal behavior in the behavioral variant of frontotemporal dementia (CB-bvFTD). This relationship was obtained in the anterior superior temporal gyrus (aSTG). (B, E) Neither negative nor positive correlation was obtained in bvFTD without criminal behavior (NoCB-bvFTD). (C, F) An interaction analysis revealed a significant group difference between bvFTD with and without criminal behavior related to the relationship between CT and FrSBe-Disinhibition. Significant clusters were obtained with p < 0.05 using family-wise error (FWE) correction for vertex-based analysis (left panel) and false discovery rate (FDR) for the region-based analysis (right panel). The dot-plot is showing CT in relationship with FrSBe-Disinhibition for both groups of bvFTD with and without criminal behavior (in red and gray color, respectively) for the global maximum within the left aSTG. L—left, R—right.

frequently in bvFTD and was related to bilateral frontomedian atrophy in the whole cohort (Phan et al. 2023). Notably, studies by Mychack et al. and Mendez et al. included subject numbers smaller than in our study. They used PET/SPECT and MRI to assess generally the laterality of the disease but did not investigate the neural correlates of CB specifically. Phan et al. included subject numbers comparable to our study, but focused on antisocial behavior and its correlates. Moreover, their finding was based on a large inhomogeneous cohort beyond bvFTD. Based on our design, that is, specifically investigating the neural correlates of CB, specific imaging methods, structural and functional MRI, and a higher number of subjects involved, we regard our results as more specific for CB.

Atrophy in right anterior temporal regions, including the amygdala and temporal pole, was reported in the context of poor emotional regulation in bvFTD (Rosen, Perry, et al. 2002), and in a more general context of neurodegenerative disease, impairment of recognition of negative facial emotional expressions was accompanied by major damage to right temporal

regions (Rosen et al. 2006). Deficits in the recognition of facial emotions, aligned with loss of empathy, might constitute a major role in the development of behavioral processes leading to CB in bvFTD. Interestingly, a prominent involvement of the right temporal lobe has been observed in patients showing reduced empathy (Hua et al. 2018; Rankin et al. 2006). The empathy score was found to be significantly correlated with gray matter volume in the right temporal lobe, right fusiform gyrus, and right frontomedian cortex (Rankin et al. 2006). These findings are in agreement with studies relating psychopathy to a greater involvement of regions within the right temporal lobe (Muller et al. 2008; Noppari et al. 2022). However, our findings in bvFTD with CB suggest an imbalance of brain atrophy between regions of the left and right temporal lobe that can impact regions in both hemispheres rather than a focused neurodegenerative process within the right hemisphere. This hypothesis is supported by findings showing the neuroanatomical correlates of disinhibition in both the left and the right temporal lobe (Schroeter et al. 2011; Sheelakumari et al. 2020). Recent work in bvFTD demonstrates a major



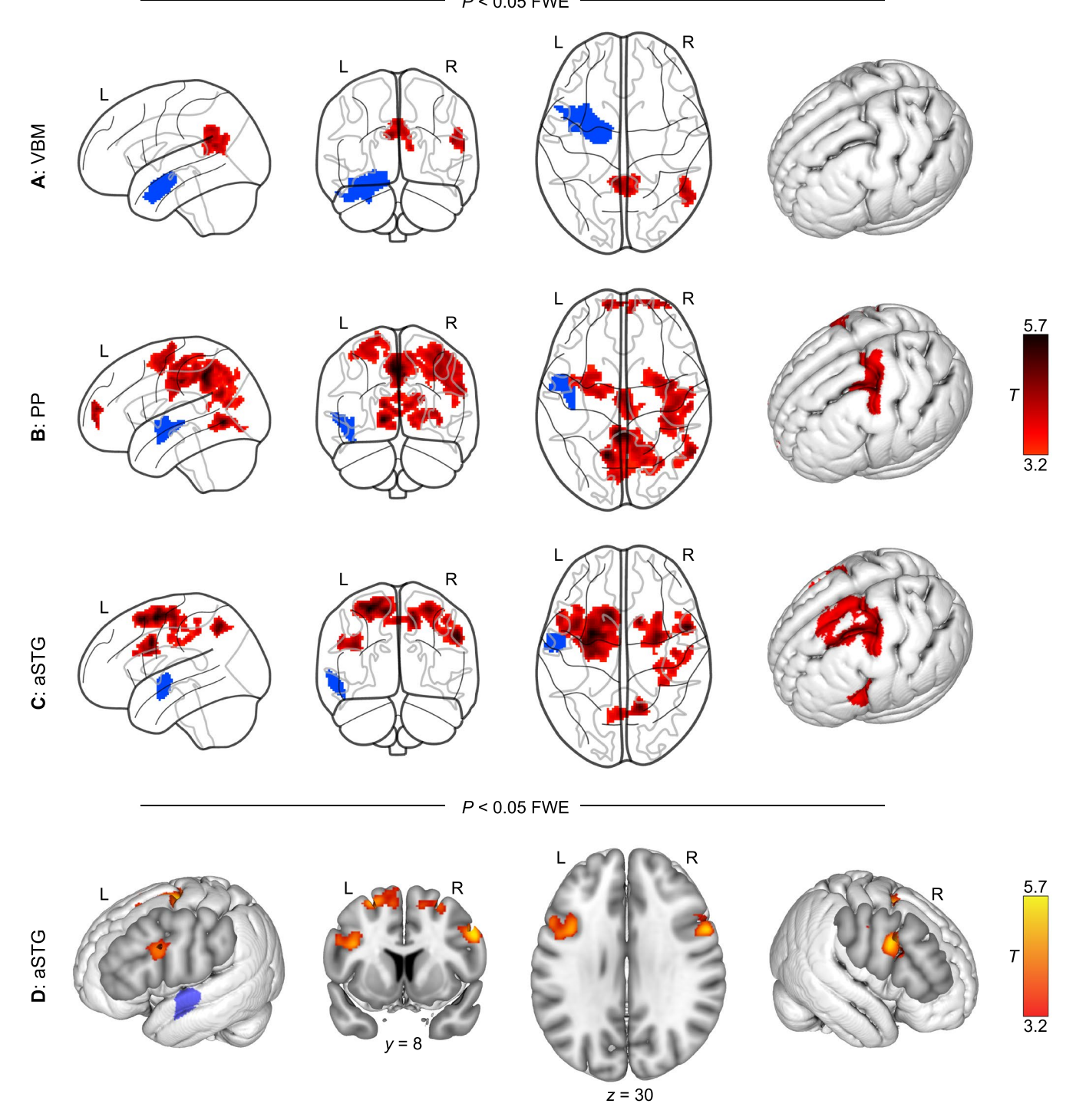
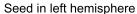


FIGURE 10 | Glass-brain views and brain sections showing functional brain connectivity decrease with criminal behavior in the behavioral variant of frontotemporal dementia (bvFTD). Comparing bvFTD with and without criminal behavior (CB-bvFTD vs. NoCB-bvFTD) using seed regions within the left temporal lobe (marked in blue color), diminished functional brain connectivity was obtained with criminal behavior between the seed region and widely distributed cortical regions including areas of the frontal and the parietal cortex. The figure shows the following seed regions in the left temporal lobe; (A) Result of voxel-based morphometry (VBM) showing a reduced gray matter density with criminal behavior (see region shown in Figure 2A); (B) Planum polare (PP); (C, D) Anterior superior temporal gyrus (aSTG). Significant differences were obtained with p < 0.05 using family-wise error (FWE) correction. L—left, R—right, y, z—coordinates in mm.

mditions) on Wiley Online Library for rules of use; OA articles are governed by the applicable Creative Commons License

10970193, 2025, 11, Downloaded from https://onlinelibrary.wiley.com/doi/10.1002/hbm.70308 by Martin Luther University Halle-Wittenberg, Wiley Online Library on [14/10/2025]. See the Terms and Conditions



Seed in right hemisphere

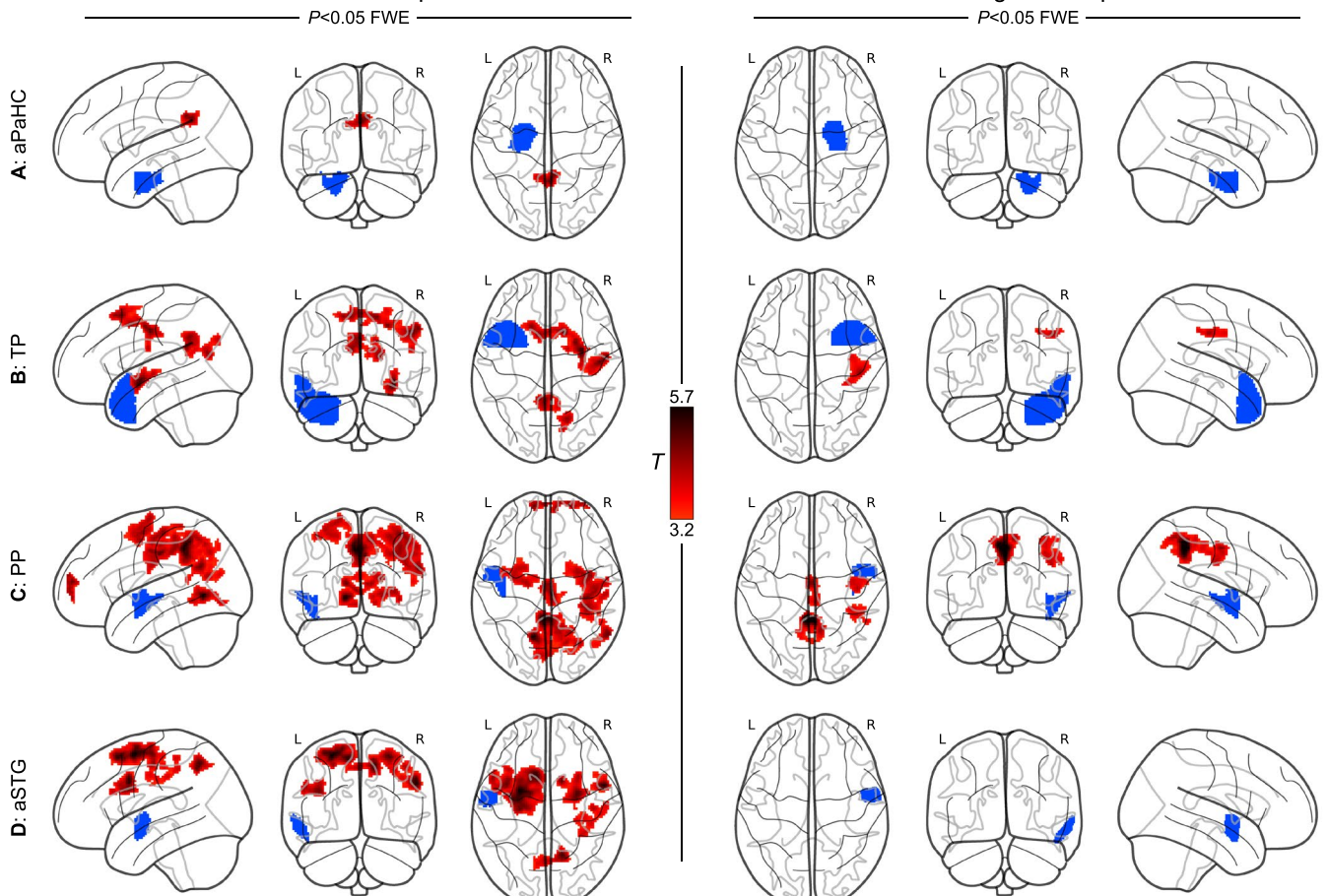


FIGURE 11 | Glass-brain views showing a functional brain connectivity decrease with criminal behavior in the behavioral variant of frontotemporal dementia (bvFTD). Comparing bvFTD with and without criminal behavior (CB-bvFTD vs. NoCB-bvFTD) using seed regions within the left temporal lobe (left panel, seed regions marked in blue color), diminished functional brain connectivity was obtained with criminal behavior between the seed region and widely distributed cortical regions including areas of the frontal and the parietal cortex. In contrast, when using seed regions within the right temporal lobe (right panel, seed regions marked in blue color), functional connectivity alterations were only detected on a minor scale. The figure shows the following seed regions in the left and right temporal lobe; (A) Anterior parahippocampal cortex (aPaHC); (B) Temporal pole (TP); (C) Planum polare (PP); (D) Anterior superior temporal gyrus (aSTG). Significant differences were obtained with p < 0.05 using family-wise error (FWE) correction. L—left, R—right.

diminishment of GMD in the left and right temporal lobe with disinhibition, that is, disinhibition correlated negatively with GMD in various regions of the temporal lobe, but also in the hippocampus and amygdala (Sheelakumari et al. 2020). We also observed a close relationship between disinhibition and brain structure in the temporal lobe, predominantly in the left anterior STG, accompanied by CB in bvFTD, thus indicating a common pattern of STG brain atrophy of disinhibition and CB in bvFTD. The relationship between disinhibition and gray matter degeneration in the left anterior STS is likely a general element in neurodegenerative disease, as this relationship was shown using structural MRI within a mixed dementia cohort where patients with Alzheimer's disease showed significantly less person-based disinhibition than in bvFTD (Paholpak et al. 2016). Interestingly, these findings show a relationship between brain structure and disinhibition in exactly the same region within the left anterior STS as obtained with our cortical thickness analysis (compare first figure in (Paholpak et al. 2016) with Figure 9A). With less degree of regional specificity, the relationship between disinhibition and temporal lobe involvement was also shown for glucose metabolism in a general context of early dementia presenting significantly higher disinhibition scores in FTD compared with Alzheimer's disease (Schroeter et al. 2011). Our result showing a significant group difference between bvFTD with and without CB with respect to the correlation between disinhibition and GMD decrease in the left anterior STG suggests that a higher degree of disinhibition accompanied by increased left temporal lobe atrophy contributes to CB in bvFTD.

4.2 | Criminal Behavior Is Associated With Reduced Functional Brain Connectivity From the Temporal Hub to Frontoparietal Brain Regions in bvFTD

In addition to our structural findings showing gray matter differences between bvFTD with and without CB, we used

functional MRI to investigate alterations in functional brain connectivity with CB when using seed-based correlation analysis defining the seed in exactly the same region within the left temporal lobe that we obtained with the VBM analysis. In addition, we used further seeds in the left and the right temporal lobe using CONN's brain parcellation. Functional brain connectivity was disturbed with CB when using the left anterior STG as the seed region. Interestingly, no significant result was obtained with the right anterior STG. Specifically, reduced connectivity was obtained with CB between the left anterior STG and widely distributed cortical regions of the frontal and prefrontal cortex, including regions within the superior frontal gyrus but also in the inferior frontal junction (IFJ). Interestingly, the IFG and particularly the IFJ play a major role in response inhibition and behavioral control (Derrfuss et al. 2005; Sundermann and Pfleiderer 2012), which might provide an internal stop signal for action related to CB (Mendez 2022). Investigating a group of 120 female prisoners with the Revisited Psychopathy Checklist, decreased IFG connectivity was found with increased antisocial scores (Yoder et al. 2022) while affective scores were related to STG dysconnectivity (Yoder et al. 2022). Reduced STG connectivity was also reported by a resting-state functional MRI study investigating 903 male prison inmates, particularly between STG and amygdala (Espinoza et al. 2019). Interestingly, comparing psychotic with nonpsychotic criminal offenders (Harenski et al. 2018), an independent component analysis revealed significantly reduced brain connectivity in the IFG and the STS in line with our findings showing a diminished brain connectivity between IFG and STS related to CB in bvFTD. In the context of emotion regulation, another recent work demonstrates significant functional brain connectivity alterations between IFG and various regions within the left temporal lobe, including the left STG between different conditions of an empathic watch paradigm (Naor et al. 2020). Considering our findings, it raises the question of whether a deficiency in empathy may contribute to the development of CB. However, loss of sympathy or empathy (diagnostic criteria for bvFTD C.1. Diminished response to people's needs and feelings, and C.2. Diminished social interest or personal warmth; see Table 2) did not differ in our two bvFTD cohorts with or without CB, making this factor rather not relevant for CB in our cohort.

The important role of the IFG was particularly studied in dementia, including a larger group of patients with Alzheimer's disease and bvFTD relating cognitive deficits-here, executive dysfunction—to hypometabolism in the IFG obtained with FDG-PET (Schroeter et al. 2012). This regional hypometabolism might reflect disrupted connectivity between the IFG and regions of the temporal lobe and suggest an involvement of executive dysfunction in CB in bvFTD. In patients with bvFTD and in agreement with our findings, dysconnectivity was shown between the anterior temporal lobe and the IFG, suggesting a reduction of a mentalizing and an action observation network combined with a reduction of emotion processing (Jastorff et al. 2016). Interestingly, the same study also showed massive gray matter atrophy in the left and right temporal lobes in the same bvFTD group that might be a contributing factor for general functional brain dysconnectivity in bvFTD. Our data suggest the same degenerative processes in bvFTD driven by the patients showing CB. Taken together,

the current literature and our findings support a general pattern of brain degeneration with a pronounced imbalance of temporal lobe atrophy leading to CB in bvFTD.

4.3 | Limitations

A significant limitation of this study is the small sample size, consisting of only 21 patients exhibiting CB in bvFTD. However, to enhance the specificity of our findings, we particularly concentrated on examining patients both with and without CB in bvFTD. Considering the rarity of CB in bvFTD, a cohort of 21 patients is a reasonably representative sample. Another major limitation of our study is the absence of a CB severity index. Although the type of CB was identified for each patient, the severity was not assessed during patient screening. Future research should incorporate a CB severity index to improve sensitivity in group analyses and to explore potential relationships between CB severity and brain structure in the left and right temporal lobes. As social cognition might be a major factor in CB, future studies should investigate further cognitive features, particularly including parameters related to social cognition.

5 | Conclusion

In comparing patients with behavioral variant frontotemporal dementia (bvFTD) who do and do not exhibit criminal behavior (CB), we observed significant brain atrophy primarily in the temporal lobes of both hemispheres, with a more pronounced effect in the left hemisphere. Our findings indicate that gray matter deterioration associated with CB, especially in cases of disinhibition, plays a crucial role. These results align with existing literature, which links disinhibition to structural changes in the brain, particularly in the temporal lobes across various dementia syndromes. Functional imaging reveals that CB in bvFTD is associated with dysconnectivity, notably manifesting as diminished connectivity between the temporal lobe and distributed regions within the frontal and parietal lobes. In summary, the most prominent structural and functional connectivity changes were observed in the left temporal lobe, prompting further investigation into the dominant role of either hemisphere. Additional research is necessary to elucidate the potential imbalance in structural and functional brain degeneration between the left and right hemispheres in bvFTD with CB.

Acknowledgments

This work was supported by the German Federal Ministry of Education and Research (BMBF) by a grant given to the German FTLD Consortium (FKZ 01GI1007A), by the German Research Foundation (DFG, SCHR 774/5-1), by the Parkinson's Disease Foundation (PDF-IRG-1307), by the Michael J. Fox Foundation (MJFF-11362), and the eHealthSax Initiative of the Sächsische Aufbaubank (SAB; project TelDem). Accordingly, this study is cofinanced with tax revenue based on the budget approved by the Saxon state parliament. Additional support was received from the EU Joint Programme Neurodegenerative Diseases networks Genfi-Prox (01ED2008A), the EU (MOODMARKER 01EW2008), the German

Research Foundation/DFG (SFB1279), the foundation of the state Baden-Württemberg (D.3830), Boehringer Ingelheim Ulm University BioCenter (D.5009), and the Thierry Latran Foundation. Open Access funding enabled and organized by Projekt DEAL.

Disclosure

Institutions involved in the study support diversity and consider it as a prerequisite for excellent science. Diversity is also mirrored in the group of participants involved in the study. In particular, there is a matched number of female and male participants in the bvFTD group (without criminal behavior) and healthy controls (see Table 1). The authors list contains contributors of all genders.

Data Availability Statement

Datasets analyzed during the current study are available on reasonable request. All data will be anonymized. MRI data will be available in preprocessed fashion (smoothed maps) in the NIfTI format without any personal meta-data. Individual GMD maps, cortical thickness maps, and seed-based correlation maps, including all group analyses, are also available. Original data are not publicly available due to privacy or ethical restrictions.

References

Andersson, J. L., C. Hutton, J. Ashburner, R. Turner, and K. Friston. 2001. "Modeling Geometric Deformations in EPI Time Series." *NeuroImage* 13, no. 5: 903–919. https://doi.org/10.1006/nimg.2001.0746.

Ashburner, J. 2007. "A Fast Diffeomorphic Image Registration Algorithm." *NeuroImage* 38, no. 1: 95–113. https://doi.org/10.1016/j.neuroimage.2007.07.007.

Ashburner, J., and K. J. Friston. 2000. "Voxel-Based Morphometry – The Methods." *NeuroImage* 11, no. 6: 805–821. https://doi.org/10.1006/nimg.2000.0582.

Ashburner, J., and K. J. Friston. 2001. "Why Voxel-Based Morphometry Should Be Used." *NeuroImage* 14, no. 6: 1238–1243. https://doi.org/10.1006/nimg.2001.0961.

Ashburner, J., and K. J. Friston. 2005. "Unified Segmentation." *NeuroImage* 26, no. 3: 839–851. https://doi.org/10.1016/j.neuroimage. 2005.02.018.

Ashburner, J., and K. J. Friston. 2011. "Diffeomorphic Registration Using Geodesic Shooting and Gauss-Newton Optimisation." *NeuroImage* 55, no. 3: 954–967. https://doi.org/10.1016/j.neuroimage.2010.12.049.

Behzadi, Y., K. Restom, J. Liau, and T. T. Liu. 2007. "A Component Based Noise Correction Method (CompCor) for BOLD and Perfusion Based fMRI." *NeuroImage* 37, no. 1: 90–101. https://doi.org/10.1016/j.neuroimage.2007.04.042.

Biswal, B., F. Z. Yetkin, V. M. Haughton, and J. S. Hyde. 1995. "Functional Connectivity in the Motor Cortex of Resting Human Brain Using Echo-Planar MRI." *Magnetic Resonance in Medicine* 34, no. 4: 537–541. https://doi.org/10.1002/mrm.1910340409.

Caceres, B. A., M. O. Frank, J. Jun, M. T. Martelly, T. Sadarangani, and P. C. de Sales. 2016. "Family Caregivers of Patients With Frontotemporal Dementia: An Integrative Review." *International Journal of Nursing Studies* 55: 71–84. https://doi.org/10.1016/j.ijnurstu.2015.10.016.

Calhoun, V. D., T. D. Wager, A. Krishnan, et al. 2017. "The Impact of T1 Versus EPI Spatial Normalization Templates for fMRI Data Analyses." *Human Brain Mapping* 38, no. 11: 5331–5342. https://doi.org/10.1002/hbm.23737.

Chai, X. J., A. N. Castanon, D. Ongur, and S. Whitfield-Gabrieli. 2012. "Anticorrelations in Resting State Networks Without Global Signal Regression." *NeuroImage* 59, no. 2: 1420–1428. https://doi.org/10.1016/j.neuroimage.2011.08.048.

Chumbley, J., K. Worsley, G. Flandin, and K. Friston. 2010. "Topological FDR for Neuroimaging." *NeuroImage* 49, no. 4: 3057–3064. https://doi.org/10.1016/j.neuroimage.2009.10.090.

Chumbley, J. R., and K. J. Friston. 2009. "False Discovery Rate Revisited: FDR and Topological Inference Using Gaussian Random Fields." *NeuroImage* 44, no. 1: 62–70. https://doi.org/10.1016/j.neuroimage.2008.05.021.

Dahnke, R., R. A. Yotter, and C. Gaser. 2013. "Cortical Thickness and Central Surface Estimation." *NeuroImage* 65: 336–348. https://doi.org/10.1016/j.neuroimage.2012.09.050.

Darby, R. R., A. Horn, F. Cushman, and M. D. Fox. 2018. "Lesion Network Localization of Criminal Behavior." *Proceedings of the National Academy of Sciences of the United States of America* 115, no. 3: 601–606. https://doi.org/10.1073/pnas.1706587115.

de Oliveira-Souza, R., R. D. Hare, I. E. Bramati, et al. 2008. "Psychopathy as a Disorder of the Moral Brain: Fronto-Temporo-Limbic Grey Matter Reductions Demonstrated by Voxel-Based Morphometry." *NeuroImage* 40, no. 3: 1202–1213. https://doi.org/10.1016/j.neuroimage.2007.12.054.

Derrfuss, J., M. Brass, J. Neumann, and D. Y. von Cramon. 2005. "Involvement of the Inferior Frontal Junction in Cognitive Control: Meta-Analyses of Switching and Stroop Studies." *Human Brain Mapping* 25, no. 1: 22–34. https://doi.org/10.1002/hbm.20127.

Desikan, R. S., F. Segonne, B. Fischl, et al. 2006. "An Automated Labeling System for Subdividing the Human Cerebral Cortex on MRI Scans Into Gyral Based Regions of Interest." *NeuroImage* 31, no. 3: 968–980. https://doi.org/10.1016/j.neuroimage.2006.01.021.

Diehl-Schmid, J., R. Perneczky, J. Koch, N. Nedopil, and A. Kurz. 2013. "Guilty by Suspicion? Criminal Behavior in Frontotemporal Lobar Degeneration." *Cognitive and Behavioral Neurology* 26, no. 2: 73–77. https://doi.org/10.1097/WNN.0b013e31829cff11.

Ermer, E., L. M. Cope, P. K. Nyalakanti, V. D. Calhoun, and K. A. Kiehl. 2012. "Aberrant Paralimbic Gray Matter in Criminal Psychopathy." *Journal of Abnormal Psychology* 121, no. 3: 649–658. https://doi.org/10.1037/a0026371.

Ermer, E., L. M. Cope, P. K. Nyalakanti, V. D. Calhoun, and K. A. Kiehl. 2013. "Aberrant Paralimbic Gray Matter in Incarcerated Male Adolescents With Psychopathic Traits." *Journal of the American Academy of Child and Adolescent Psychiatry* 52, no. 1: 94–103. https://doi.org/10.1016/j.jaac.2012.10.013.

Espinoza, F. A., N. E. Anderson, V. M. Vergara, et al. 2019. "Resting-State fMRI Dynamic Functional Network Connectivity and Associations With Psychopathy Traits." *Neuroimage Clin* 24: 101970. https://doi.org/10.1016/j.nicl.2019.101970.

Fischl, B., M. I. Sereno, R. B. Tootell, and A. M. Dale. 1999. "High-Resolution Intersubject Averaging and a Coordinate System for the Cortical Surface." *Human Brain Mapping* 8, no. 4: 272–284. https://doi.org/10.1002/(sici)1097-0193(1999)8:4<272::aid-hbm10>3.0.co;2-4.

Flandin, G., and K. J. Friston. 2019. "Analysis of Family-Wise Error Rates in Statistical Parametric Mapping Using Random Field Theory." *Human Brain Mapping* 40, no. 7: 2052–2054. https://doi.org/10.1002/hbm.23839.

Friston, K. J., J. Ashburner, C. D. Frith, J. B. Poline, J. D. Heather, and R. S. Frackowiak. 1995. "Spatial Registration and Normalization of Images." *Human Brain Mapping* 3, no. 3: 165–189.

Friston, K. J., J. T. Ashburner, S. J. Kiebel, T. E. Nichols, and W. D. Penny. 2007. *Statistical Parametric Mapping: The Analysis of Functional Brain Images*. Academic Press. https://doi.org/10.1016/B978-0-12-37256 0-8.X5000-1.

Friston, K. J., S. Williams, R. Howard, R. S. Frackowiak, and R. Turner. 1996. "Movement-Related Effects in fMRI Time-Series." *Magnetic Resonance in Medicine* 35, no. 3: 346–355. https://doi.org/10.1002/mrm. 1910350312.

Friston, K. J., K. J. Worsley, R. S. Frackowiak, J. C. Mazziotta, and A. C. Evans. 1994. "Assessing the Significance of Focal Activations Using Their Spatial Extent." *Human Brain Mapping* 1, no. 3: 210–220. https://doi.org/10.1002/hbm.460010306.

Gaser, C., R. Dahnke, P. M. Thompson, F. Kurth, and E. Luders. 2023. "CAT – A Computational Anatomy Toolbox for the Analysis of Structural MRI Data." bioRxiv, 2022.2006.2011.495736. https://doi.org/10.1101/2022.06.11.495736.

Gatzke-Kopp, L. M., A. Raine, M. Buchsbaum, and L. LaCasse. 2001. "Temporal Lobe Deficits in Murderers: EEG Findings Undetected by PET." *Journal of Neuropsychiatry and Clinical Neurosciences* 13, no. 4: 486–491. https://doi.org/10.1176/jnp.13.4.486.

Glascher, J., and D. Gitelman. 2008. "Contrast Weights in Flexible Factorial Design With Multiple Groups of Subjects."

Gonzalez-Alemany, E., A. D. Rodriguez Olivera, M. A. Bobes, and J. L. Armony. 2023. "Brain Structural Correlates of Psychopathic Traits in Elite Female Combat-Sports Athletes." *European Journal of Neuroscience* 58, no. 10: 4255–4263. https://doi.org/10.1111/ejn.16171.

Gorno-Tempini, M. L., A. E. Hillis, S. Weintraub, et al. 2011. "Classification of Primary Progressive Aphasia and Its Variants." *Neurology* 76, no. 11: 1006–1014. https://doi.org/10.1212/WNL.0b013e31821103e6.

Grace, J., and P. F. Malloy. 2020. "Frontal Systems Behavior Scale (FrSBe)." In *A Compendium of Tests, Scales and Questionnaires*, edited by R. L. Tate, 316–318. Psychology Press. https://doi.org/10.4324/9781003076391-81.

Hallquist, M. N., K. Hwang, and B. Luna. 2013. "The Nuisance of Nuisance Regression: Spectral Misspecification in a Common Approach to Resting-State fMRI Preprocessing Reintroduces Noise and Obscures Functional Connectivity." *NeuroImage* 82: 208–225. https://doi.org/10.1016/j.neuroimage.2013.05.116.

Harenski, C. L., V. D. Calhoun, J. R. Bustillo, et al. 2018. "Functional Connectivity During Affective Mentalizing in Criminal Offenders With Psychotic Disorders: Associations With Clinical Symptoms." *Psychiatry Research: Neuroimaging* 271: 91–99. https://doi.org/10.1016/j.pscychresns.2017.11.003.

Hofhansel, L., C. Weidler, M. Votinov, B. Clemens, A. Raine, and U. Habel. 2020. "Morphology of the Criminal Brain: Gray Matter Reductions Are Linked to Antisocial Behavior in Offenders." *Brain Structure & Function* 225, no. 7: 2017–2028. https://doi.org/10.1007/s00429-020-02106-6.

Hua, A. Y., I. J. Sible, D. C. Perry, et al. 2018. "Enhanced Positive Emotional Reactivity Undermines Empathy in Behavioral Variant Frontotemporal Dementia." *Frontiers in Neurology* 9: 402. https://doi.org/10.3389/fneur.2018.00402.

Jastorff, J., F. L. De Winter, J. Van den Stock, R. Vandenberghe, M. A. Giese, and M. Vandenbulcke. 2016. "Functional Dissociation Between Anterior Temporal Lobe and Inferior Frontal Gyrus in the Processing of Dynamic Body Expressions: Insights From Behavioral Variant Frontotemporal Dementia." *Human Brain Mapping* 37, no. 12: 4472–4486. https://doi.org/10.1002/hbm.23322.

Kiebel, S., and K. Mueller. 2015. "The General Linear Model." In *Brain Mapping*, edited by A. W. Toga, vol. 1, 465–469. Academic Press. https://doi.org/10.1016/B978-0-12-397025-1.00317-1.

Kiehl, K. A., A. M. Smith, A. Mendrek, B. B. Forster, R. D. Hare, and P. F. Liddle. 2004. "Temporal Lobe Abnormalities in Semantic Processing by Criminal Psychopaths as Revealed by Functional Magnetic Resonance Imaging." *Psychiatry Research* 130, no. 3: 297–312. https://doi.org/10.1016/j.pscychresns.2004.02.002.

Kipps, C. M., R. R. Davies, J. Mitchell, J. J. Kril, G. M. Halliday, and J. R. Hodges. 2007. "Clinical Significance of Lobar Atrophy in Frontotemporal Dementia: Application of an MRI Visual Rating Scale." *Dementia and Geriatric Cognitive Disorders* 23, no. 5: 334–342. https://doi.org/10.1159/000100973.

Kolla, N. J., S. Gregory, S. Attard, N. Blackwood, and S. Hodgins. 2014. "Disentangling Possible Effects of Childhood Physical Abuse on Gray Matter Changes in Violent Offenders With Psychopathy." *Psychiatry Research* 221, no. 2: 123–126. https://doi.org/10.1016/j.pscychresns. 2013.11.008.

Leutgeb, V., M. Leitner, A. Wabnegger, et al. 2015. "Brain Abnormalities in High-Risk Violent Offenders and Their Association With Psychopathic Traits and Criminal Recidivism." *Neuroscience* 308: 194–201. https://doi.org/10.1016/j.neuroscience.2015.09.011.

Liljegren, M., M. Landqvist Waldo, A. Frizell Santillo, et al. 2019. "Association of Neuropathologically Confirmed Frontotemporal Dementia and Alzheimer Disease With Criminal and Socially Inappropriate Behavior in a Swedish Cohort." *JAMA Network Open* 2, no. 3: e190261. https://doi.org/10.1001/jamanetworkopen.2019.0261.

Ly, M., J. C. Motzkin, C. L. Philippi, et al. 2012. "Cortical Thinning in Psychopathy." *American Journal of Psychiatry* 169, no. 7: 743–749. https://doi.org/10.1176/appi.ajp.2012.11111627.

Manjon, J. V., P. Coupe, L. Marti-Bonmati, D. L. Collins, and M. Robles. 2010. "Adaptive Non-Local Means Denoising of MR Images With Spatially Varying Noise Levels." *Journal of Magnetic Resonance Imaging* 31, no. 1: 192–203. https://doi.org/10.1002/jmri.22003.

Mansfield, P., R. Coxon, and P. Glover. 1994. "Echo-Planar Imaging of the Brain at 3.0 T: First Normal Volunteer Results." *Journal of Computer Assisted Tomography* 18, no. 3: 339–343. https://doi.org/10.1097/00004728-199405000-00001.

Mendez, M. F. 2022. "Behavioral Variant Frontotemporal Dementia and Social and Criminal Transgressions." *Journal of Neuropsychiatry and Clinical Neurosciences* 34, no. 4: 328–340. https://doi.org/10.1176/appi.neuropsych.21080224.

Mendez, M. F., E. Anderson, and J. S. Shapira. 2005. "An Investigation of Moral Judgement in Frontotemporal Dementia." *Cognitive and Behavioral Neurology* 18, no. 4: 193–197. https://doi.org/10.1097/01.wnn.0000191292.17964.bb.

Mendez, M. F., A. K. Chen, J. S. Shapira, and B. L. Miller. 2005. "Acquired Sociopathy and Frontotemporal Dementia." *Dementia and Geriatric Cognitive Disorders* 20, no. 2–3: 99–104. https://doi.org/10. 1159/000086474.

Meyer, S., K. Mueller, K. Stuke, et al. 2017. "Predicting Behavioral Variant Frontotemporal Dementia With Pattern Classification in Multi-Center Structural MRI Data." *Neuroimage Clin* 14: 656–662. https://doi.org/10.1016/j.nicl.2017.02.001.

Morris, J. C., A. Heyman, R. C. Mohs, et al. 1989. "The Consortium to Establish a Registry for Alzheimer's Disease (CERAD). Part I. Clinical and Neuropsychological Assessment of Alzheimer's Disease." *Neurology* 39, no. 9: 1159. https://doi.org/10.1212/wnl.39.9.1159.

Mugler, J. P., 3rd, and J. R. Brookeman. 1991. "Rapid Three-Dimensional T1-Weighted MR Imaging With the MP-RAGE Sequence." *Journal of Magnetic Resonance Imaging* 1, no. 5: 561–567. https://doi.org/10.1002/jmri.1880010509.

Muller, J. L., S. Ganssbauer, M. Sommer, et al. 2008. "Gray Matter Changes in Right Superior Temporal Gyrus in Criminal Psychopaths. Evidence From Voxel-Based Morphometry." *Psychiatry Research* 163, no. 3: 213–222. https://doi.org/10.1016/j.pscychresns. 2007.08.010.

Mychack, P., J. H. Kramer, K. B. Boone, and B. L. Miller. 2001. "The Influence of Right Frontotemporal Dysfunction on Social Behavior in Frontotemporal Dementia." *Neurology* 56, no. 11: S11–S15. https://doi.org/10.1212/wnl.56.suppl_4.s11.

Naor, N., C. Rohr, L. H. Schaare, C. Limbachia, S. Shamay-Tsoory, and H. Okon-Singer. 2020. "The Neural Networks Underlying Reappraisal of Empathy for Pain." *Social Cognitive and Affective Neuroscience* 15, no. 7: 733–744. https://doi.org/10.1093/scan/nsaa094.

Nieto-Castanon, A. 2020a. "FMRI Denoising Pipeline." In Handbook of Functional Connectivity Magnetic Resonance Imaging Methods in CONN, 17–25. Hilbert Press.

Nieto-Castanon, A. 2020b. "FMRI Minimal Preprocessing Pipeline." In *Handbook of Functional Connectivity Magnetic Resonance Imaging Methods in CONN*, 3–16. Hilbert Press.

Nieto-Castanon, A. 2020c. "Functional Connectivity Measures." In *Handbook of Functional Connectivity Magnetic Resonance Imaging Methods in CONN*, edited by A. Nieto-Castanon, 26–62. Hilbert Press.

Nieto-Castanon, A. 2022. "Preparing fMRI Data for Statistical Analysis." arXiv, 2210.13564. https://arxiv.org/pdf/2210.13564.pdf.

Nieto-Castanon, A., and S. Whitfield-Gabrieli. 2022. CONN Functional Connectivity Toolbox: RRID SCR 009550, Release 22. Hilbert Press.

Noppari, T., L. Sun, L. Lukkarinen, et al. 2022. "Brain Structural Alterations in Autism and Criminal Psychopathy." *Neuroimage Clin* 35: 103116. https://doi.org/10.1016/j.nicl.2022.103116.

Otto, M., A. C. Ludolph, B. Landwehrmeyer, et al. 2011. "German Consortium for Frontotemporal Lobar Degeneration." *Nervenarzt* 82, no. 8: 1002–1005. https://doi.org/10.1007/s00115-011-3261-3.

Paholpak, P., A. R. Carr, J. P. Barsuglia, et al. 2016. "Person-Based Versus Generalized Impulsivity Disinhibition in Frontotemporal Dementia and Alzheimer Disease." *Journal of Geriatric Psychiatry and Neurology* 29, no. 6: 344–351. https://doi.org/10.1177/0891988716666377.

Patrick, C. J. 2008. "Psychophysiological Correlates of Aggression and Violence: An Integrative Review." *Philosophical Transactions of the Royal Society of London. Series B, Biological Sciences* 363, no. 1503: 2543–2555. https://doi.org/10.1098/rstb.2008.0028.

Phan, T. X., J. E. Reeder, L. C. Keener, et al. 2023. "Measuring Antisocial Behaviors in Behavioral Variant Frontotemporal Dementia With a Novel Informant-Based Questionnaire." *Journal of Neuropsychiatry and Clinical Neurosciences* 35, no. 4: 374–384. https://doi.org/10.1176/appi.neuropsych.20220135.

Power, J. D., A. Mitra, T. O. Laumann, A. Z. Snyder, B. L. Schlaggar, and S. E. Petersen. 2014. "Methods to Detect, Characterize, and Remove Motion Artifact in Resting State fMRI." *NeuroImage* 84: 320–341. https://doi.org/10.1016/j.neuroimage.2013.08.048.

Rajapakse, J. C., J. N. Giedd, and J. L. Rapoport. 1997. "Statistical Approach to Segmentation of Single-Channel Cerebral MR Images." *IEEE Transactions on Medical Imaging* 16, no. 2: 176–186. https://doi.org/10.1109/42.563663.

Rankin, K. P., M. L. Gorno-Tempini, S. C. Allison, et al. 2006. "Structural Anatomy of Empathy in Neurodegenerative Disease." *Brain* 129, no. Pt 11: 2945–2956. https://doi.org/10.1093/brain/awl254.

Rascovsky, K., J. R. Hodges, D. Knopman, et al. 2011. "Sensitivity of Revised Diagnostic Criteria for the Behavioural Variant of Frontotemporal Dementia." *Brain* 134, no. Pt 9: 2456–2477. https://doi.org/10.1093/brain/awr179.

Rosen, H. J., S. C. Allison, G. F. Schauer, M. L. Gorno-Tempini, M. W. Weiner, and B. L. Miller. 2005. "Neuroanatomical Correlates of Behavioural Disorders in Dementia." *Brain* 128, no. 11: 2612–2625. https://doi.org/10.1093/brain/awh628.

Rosen, H. J., M. L. Gorno-Tempini, W. P. Goldman, et al. 2002. "Patterns of Brain Atrophy in Frontotemporal Dementia and Semantic Dementia." *Neurology* 58, no. 2: 198–208. https://doi.org/10.1212/wnl.58.2.198.

Rosen, H. J., R. J. Perry, J. Murphy, et al. 2002. "Emotion Comprehension in the Temporal Variant of Frontotemporal Dementia." *Brain* 125, no. 10: 2286–2295. https://doi.org/10.1093/brain/awf225.

Rosen, H. J., M. R. Wilson, G. F. Schauer, et al. 2006. "Neuroanatomical Correlates of Impaired Recognition of Emotion in Dementia." *Neuropsychologia* 44, no. 3: 365–373. https://doi.org/10.1016/j.neuropsychologia.2005.06.012.

Sato, J. R., R. de Oliveira-Souza, C. E. Thomaz, et al. 2011. "Identification of Psychopathic Individuals Using Pattern Classification of MRI Images." *Social Neuroscience* 6, no. 6: 627–639. https://doi.org/10.1080/17470919.2011.562687.

Schroeter, M. L., A. R. Laird, C. Chwiesko, et al. 2014. "Conceptualizing Neuropsychiatric Diseases With Multimodal Data-Driven Meta-Analyses - The Case of Behavioral Variant Frontotemporal Dementia." *Cortex* 57: 22–37. https://doi.org/10.1016/j.cortex.2014.02.022.

Schroeter, M. L., B. Vogt, S. Frisch, et al. 2011. "Dissociating Behavioral Disorders in Early Dementia-An FDG-PET Study." *Psychiatry Research* 194, no. 3: 235–244. https://doi.org/10.1016/j.pscychresns.2011.06.009.

Schroeter, M. L., B. Vogt, S. Frisch, et al. 2012. "Executive Deficits Are Related to the Inferior Frontal Junction in Early Dementia." *Brain* 135, no. 1: 201–215. https://doi.org/10.1093/brain/awr311.

Seeley, W. W. 2008. "Selective Functional, Regional, and Neuronal Vulnerability in Frontotemporal Dementia." *Current Opinion in Neurology* 21, no. 6: 701–707. https://doi.org/10.1097/WCO.0b013e3283 168e2d.

Shattuck, D. W., M. Mirza, V. Adisetiyo, et al. 2008. "Construction of a 3D Probabilistic Atlas of Human Cortical Structures." *NeuroImage* 39, no. 3: 1064–1080. https://doi.org/10.1016/j.neuroimage.2007.09.031.

Sheelakumari, R., C. Bineesh, T. Varghese, C. Kesavadas, J. Verghese, and P. S. Mathuranath. 2020. "Neuroanatomical Correlates of Apathy and Disinhibition in Behavioural Variant Frontotemporal Dementia." *Brain Imaging and Behavior* 14, no. 5: 2004–2011. https://doi.org/10.1007/s11682-019-00150-3.

Shinagawa, S., K. Shigenobu, K. Tagai, et al. 2017. "Violation of Laws in Frontotemporal Dementia: A Multicenter Study in Japan." *Journal of Alzheimer's Disease* 57, no. 4: 1221–1227. https://doi.org/10.3233/JAD-170028.

Stehling, M. K., R. Turner, and P. Mansfield. 1991. "Echo-Planar Imaging: Magnetic Resonance Imaging in a Fraction of a Second." *Science* 254, no. 5028: 43–50. https://doi.org/10.1126/science.1925560.

Stout, J. C., R. E. Ready, J. Grace, P. F. Malloy, and J. S. Paulsen. 2003. "Factor Analysis of the Frontal Systems Behavior Scale (FrSBe)." *Assessment* 10, no. 1: 79–85. https://doi.org/10.1177/1073191102 250339.

Sundermann, B., and B. Pfleiderer. 2012. "Functional Connectivity Profile of the Human Inferior Frontal Junction: Involvement in a Cognitive Control Network." *BMC Neuroscience* 13: 119. https://doi.org/10.1186/1471-2202-13-119.

Tohka, J., A. Zijdenbos, and A. Evans. 2004. "Fast and Robust Parameter Estimation for Statistical Partial Volume Models in Brain MRI." *NeuroImage* 23, no. 1: 84–97. https://doi.org/10.1016/j.neuroimage.2004.05.007.

Ulugut, H., M. Bertoux, K. Younes, et al. 2024. "Clinical Recognition of Frontotemporal Dementia With Right Anterior Temporal Predominance: A Multicenter Retrospective Cohort Study." *Alzheimers Dement* 20, no. 8: 5647–5661. https://doi.org/10.1002/alz.14076.

Vieira, J. B., F. Ferreira-Santos, P. R. Almeida, F. Barbosa, J. Marques-Teixeira, and A. A. Marsh. 2015. "Psychopathic Traits Are Associated With Cortical and Subcortical Volume Alterations in Healthy Individuals." *Social Cognitive and Affective Neuroscience* 10, no. 12: 1693–1704. https://doi.org/10.1093/scan/nsv062.

Weise, C. M., A. Engel, M. Polyakova, et al. 2024. "Dissecting Neural Correlates of Theory of Mind and Executive Functions in Behavioral Variant Frontotemporal Dementia." *Alzheimer's Research & Therapy* 16, no. 1: 237. https://doi.org/10.1186/s13195-024-01596-4.

Whitfield-Gabrieli, S., and A. Nieto-Castanon. 2012. "Conn: A Functional Connectivity Toolbox for Correlated and Anticorrelated Brain Networks." *Brain Connectivity* 2, no. 3: 125–141. https://doi.org/10.1089/brain.2012.0073.

Whitfield-Gabrieli, S., A. Nieto-Castanon, and S. Ghosh. 2011. "Artifact Detection Tools (ART)." Release Version 7(19).

Whitwell, J. L. 2019. "FTD Spectrum: Neuroimaging Across the FTD Spectrum." *Progress in Molecular Biology and Translational Science* 165: 187–223. https://doi.org/10.1016/bs.pmbts.2019.05.009.

Worsley, K. J., S. Marrett, P. Neelin, A. C. Vandal, K. J. Friston, and A. C. Evans. 1996. "A Unified Statistical Approach for Determining Significant Signals in Images of Cerebral Activation." *Human Brain Mapping* 4, no. 1: 58–73. https://doi.org/10.1002/(SICI)1097-0193(1996)4:1<58::AID-HBM4>3.0.CO;2-O.

Yoder, K. J., C. L. Harenski, K. A. Kiehl, and J. Decety. 2022. "Psychopathic Traits Modulate Functional Connectivity During Pain Perception and Perspective-Taking in Female Inmates." *Neuroimage Clin* 34: 102984. https://doi.org/10.1016/j.nicl.2022.102984.

Yotter, R. A., R. Dahnke, P. M. Thompson, and C. Gaser. 2011. "Topological Correction of Brain Surface Meshes Using Spherical Harmonics." *Human Brain Mapping* 32, no. 7: 1109–1124. https://doi.org/10.1002/hbm.21095.

Yotter, R. A., I. Nenadic, G. Ziegler, P. M. Thompson, and C. Gaser. 2011. "Local Cortical Surface Complexity Maps From Spherical Harmonic Reconstructions." *NeuroImage* 56, no. 3: 961–973. https://doi.org/10.1016/j.neuroimage.2011.02.007.

Supporting Information

Additional supporting information can be found online in the Supporting Information section. Figure S1: Voxel- and vertex-based analysis showing decreased gray matter density (GMD) and cortical thickness with criminal behavior in the behavioral variant of frontotemporal dementia (bvFTD) including disease severity (clinical dementia rate, CDR) as an additional covariate in the statistical model. For details, see Figures 2A and 3A. Figure S2: Voxel-based analysis showing gray matter density (GMD) decrease with criminal behavior in the behavioral variant of frontotemporal dementia (bvFTD) including years of education as an additional covariate in the statistical model. For details, see Figure 2A-C. Figure S3: Vertex-based analysis showing decreased cortical thickness with criminal behavior in the behavioral variant of frontotemporal dementia (bvFTD) including years of education as an additional covariate in the statistical model. For details, see Figure 3A-C. Figure S4: Glass-brain views showing functional brain connectivity decrease with criminal behavior in the behavioral variant of frontotemporal dementia (bvFTD) including years of education as an additional covariate in the statistical model. For details, see Figure 10. Figure S5: Glass-brain views showing functional brain connectivity decrease with criminal behavior in the behavioral variant of frontotemporal dementia (bvFTD) accounting for gray matter loss in the left temporal lobe. Accounting for gray matter loss was performed using an additional confounding covariate in the statistical model including gray matter density values in the maximum of the cluster shown in Figure 2A. For details, see Figure 10. Figure S6: Glass-brain views showing functional brain connectivity decrease with criminal behavior in the behavioral variant of frontotemporal dementia (bvFTD) accounting for gray matter loss in the left temporal lobe. Accounting for gray matter loss was performed using an additional confounding covariate in the statistical model including the first eigenvariate of gray matter density values within the cluster shown in Figure 2A. For details, see Figure 10.